Testing lepton flavour universality in semileptonic $\Lambda_b \to \Lambda_c^*$ decays

Böer, Philipp ; Bordone, Marzia ; Graverini, Elena ; Owen, Patrick ; Rotondo, Marcello ; van Dyk, Danny

Abstract: Lepton Flavour Universality tests with semileptonic Λb → Λ c * decays are important to corroborate the present anomalies in the similar ratios RD(∗), and can provide complementary constraints on possible origins of these anomalies beyond the Standard Model. In this paper we provide — for the first time — all the necessary theoretical ingredients to perform and interpret measurements of RΛ∗c at the LHCb experiment. For this, we revisit the heavy-quark expansion of the relevant hadronic matrix elements, and provide their expressions to order s and 1/m accuracy. Moreover, we study the sensitivity to the form factor parameters given the projected size and purity of upcoming and future LHCb datasets of Λb→Λ∗c ¯¯¯ decays. We demonstrate explicitly the need to perform a simultaneous fit to both Λ c * final states. Finally, we provide projections for the uncertainty of RΛ∗c based on the form factors analysis from semimuonic decays and theoretical relations based on the heavy-quark expansion.

DOI: https://doi.org/10.1007/jhep06(2018)155

Published for SISSA by Springer

Received: February 5, 2018
Revised: May 31, 2018
Accepted: June 7, 2018
Published: June 27, 2018

Testing lepton flavour universality in semileptonic $\Lambda_b \to \Lambda_c^*$ decays

Philipp Böer,[a] **Marzia Bordone,**[b] **Elena Graverini,**[b] **Patrick Owen,**[b] **Marcello Rotondo**[c] **and Danny van Dyk**[b,d]

[a] *Theoretische Physik 1, Naturwissenschaftlich-Technische Fakultät, Universität Siegen, Walter-Flex-Straße 3, D-57068 Siegen, Germany*

[b] *Physik Institut, Universität Zürich, Winterthurerstrasse 190, CH-8057 Zürich, Switzerland*

[c] *Laboratori Nazionali dell'INFN di Frascati, Frascati, Italy*

[d] *Physik Department, Technische Universität München, James-Franck-Straße 1, D-85748 Garching, Germany*

E-mail: boeer@physik.uni-siegen.de, mbordone@physik.uzh.ch, elena.graverini@cern.ch, powen@physik.uzh.ch, marcello.rotondo@cern.ch, danny.van.dyk@gmail.com

Abstract: Lepton Flavour Universality tests with semileptonic $\Lambda_b \to \Lambda_c^*$ decays are important to corroborate the present anomalies in the similar ratios $R_{D^{(*)}}$, and can provide complementary constraints on possible origins of these anomalies beyond the Standard Model. In this paper we provide — for the first time — all the necessary theoretical ingredients to perform and interpret measurements of $R_{\Lambda_c^*}$ at the LHCb experiment. For this, we revisit the heavy-quark expansion of the relevant hadronic matrix elements, and provide their expressions to order α_s and $1/m$ accuracy. Moreover, we study the sensitivity to the form factor parameters given the projected size and purity of upcoming and future LHCb datasets of $\Lambda_b \to \Lambda_c^* \mu \bar{\nu}$ decays. We demonstrate explicitly the need to perform a simultaneous fit to both Λ_c^* final states. Finally, we provide projections for the uncertainty of $R_{\Lambda_c^*}$ based on the form factors analysis from semimuonic decays and theoretical relations based on the heavy-quark expansion.

Keywords: Heavy Quark Physics, Beyond Standard Model

ArXiv ePrint: 1801.08367

https://doi.org/10.1007/JHEP06(2018)155

JHEP06(2018)155

Contents

1 Introduction

Tests of lepton flavour universality in semileptonic decays of b quarks are presently in focus of both experimental as well as theoretical particle physics. This interest has been sparked by deviations between Standard Model (SM) estimates and measurements in both

JHEP06(2018)155

charged-current [1–9] and neutral-current [10, 11] semileptonic b quark decays. Deviations in both sectors are at the level of three to four standard deviations, which is at present intriguing but does not yet provide conclusive evidence for particles beyond the SM. It is therefore important to extend the current tests to new decay modes to provide measurements with orthogonal experimental and theoretical systematic uncertainties as well as a complementary sensitivity to new physics.

In this paper we will concentrate on Lepton Flavour Universality (LFU) in $b \to c\tau\bar{\nu}$ versus $b \to c\mu\bar{\nu}$ decays, in particular for Λ_b^0 decays. At the LHC, Λ_b^0 baryons are copiously produced, at approximately half the rate of B^0 mesons [12, 13]. The decay involving the ground state charmed baryon, $\Lambda_b^0 \to \Lambda_c^+ \ell^- \bar{\nu}$ has been studied in lattice QCD in ref. [14] and precise predictions for the LFU ratio R_{Λ_c} are provided in the SM and beyond [14, 15]. In addition, the LHCb collaboration has recently measured the slope of the leading order Isgur-Wise (IW) function of the decay $\Lambda_b^0 \to \Lambda_c^+ \mu^- \bar{\nu}$ [16]. While studying backgrounds to this decay, large samples of $\Lambda_c(2595)^+$ and $\Lambda_c(2625)^+$ candidates were reconstructed as background, which demonstrates the potential of precise LFU tests in these decays. Therefore, we propose to investigate the LFU ratios

$$R_{\Lambda_c^*} \equiv \frac{\mathcal{B}(\Lambda_b^0 \to \Lambda_c^{*+} \tau^- \bar{\nu})}{\mathcal{B}(\Lambda_b^0 \to \Lambda_c^{*+} \mu^- \bar{\nu})} \tag{1.1}$$

where Λ_c^{*+} denotes either the $\Lambda_c(2595)^+$ (with $J^P = 1/2^-$) or the $\Lambda_c(2625)^+$ (with $J^P = 3/2^-$) charmed baryon.

The challenge in exploiting these modes for LFU tests is controlling uncertainties related to the hadronic matrix elements, which are genuinely non-perturbative objects. As a consequence of both baryons forming a doublet under Heavy Quark Spin Symmetry (HQSS), the hadronic matrix elements for the $\Lambda_b \to \Lambda_c^*$ transitions can be expressed — in the infinite mass limit — through a single IW function ζ [17] at leading power in $1/m$. The power suppressed contributions at the $1/m$ level — where $m = m_b, m_c$ — have been previously calculated in [18].

The purpose of this paper is to provide for the first time all the necessary ingredients to carry out a LFU study of these decays. In section 2, we first revisit the definition of the hadronic form factors, and provide a helicity decomposition that is convenient for the description of the decay observables. Subsequently, we provide formulae for these hadronic form factors in the Heavy Quark Expansion (HQE) up to order α_s and $1/m$, beyond what has been done in the literature so far. Continuing in section 3, we model the kinematic dependence of the leading and subleading IW functions, and then provide a set of benchmark points based on inputs from non-perturbative approaches. Afterwards, we calculate the differential decay width, including the finite lepton-mass contributions that are necessary for testing LFU. The following section 4 shows the impact of using LHCb data for constraining the relevant form factor parameters, and control the theory uncertainties for the prediction of the LFU ratios. We conclude in section 5.

JHEP06(2018)155

2 Form factors for $\Lambda_b \to \Lambda_c^*$ transitions

In the following we investigate form factors for the transitions

$$\Lambda_b^0(p, s_b) \to \begin{cases} \Lambda_c(2595)^+(k, J_z \equiv s_c) & \text{with } J^P = 1/2^- \\ \Lambda_c(2625)^+(k, J_z \equiv s_c + \lambda_c) & \text{with } J^P = 3/2^- \end{cases}, \tag{2.1}$$

where p and k denote the four momenta of the initial and final state respectively, and J^P indicates both angular momentum and parity eigenvalues of the Λ_c^{*+} states. The states' rest-frame helicities are denoted as s_b and J_z. Note that, for the $J^P = 3/2^-$ state, J_z can be decomposed into the rest-frame helicity of a $1/2^+$ spinor (s_c), and the polarisation of a polarisation vector $\eta \equiv \eta(\lambda_c)$. For later use we also define the momentum transfer to the leptons $q^\mu \equiv p^\mu - k^\mu$.

2.1 Helicity form factors

We define the hadronic matrix elements for vector and axialvector transitions to the $\Lambda_c(2595)^+$ state as:

$$\begin{aligned} \langle \Lambda_c(2595)^+(k,\eta(\lambda_c),s_c)|\,\bar{c}\gamma^\mu b\,|\Lambda_b^0(p,s_b)\rangle &= +\bar{u}_\alpha^{(1/2)}(k,\eta(\lambda_c),s_c)\left[\sum_i f_i(q^2)\Gamma_{V,i}^{\alpha\mu}\right]u(p,s_b)\,, \\ \langle \Lambda_c(2595)^+(k,\eta(\lambda_c),s_c)|\,\bar{c}\gamma^\mu\gamma_5 b\,|\Lambda_b^0(p,s_b)\rangle &= -\bar{u}_\alpha^{(1/2)}(k,\eta(\lambda_c),s_c)\left[\sum_i g_i(q^2)\gamma_5\Gamma_{A,i}^{\alpha\mu}\right]u(p,s_b)\,, \end{aligned} \tag{2.2}$$

where $\bar{u}_\alpha^{(1/2)}$ is the spin 1/2 projection of a Rarita-Schwinger object $u_\alpha^{\mathrm{RS}}(k,\eta,s) \equiv \eta_\alpha(k)u(k,s)$ (see appendix A). For the hadronic matrix element of the vector and axialvector transitions to the $\Lambda_c(2625)^+$ state we use:

$$\begin{aligned} \langle \Lambda_c(2625)^+(k,\eta(\lambda_c),s_c)|\,\bar{c}\gamma^\mu b\,|\Lambda_b^0(p,s_b)\rangle &= +\bar{u}_\alpha^{(3/2)}(k,\eta(\lambda_c),s_c)\left[\sum_i F_i(q^2)\Gamma_{V,i}^{\alpha\mu}\right]u(p,s_b)\,, \\ \langle \Lambda_c(2625)^+(k,\eta(\lambda_c),s_c)|\,\bar{c}\gamma^\mu\gamma_5 b\,|\Lambda_b^0(p,s_b)\rangle &= -\bar{u}_\alpha^{(3/2)}(k,\eta(\lambda_c),s_c)\left[\sum_i G_i(q^2)\gamma_5\Gamma_{A,i}^{\alpha\mu}\right]u(p,s_b)\,, \end{aligned} \tag{2.3}$$

where $\bar{u}_\alpha^{(3/2)}$ is the spin 3/2 projection of a Rarita-Schwinger object; see also appendix A. A possible basis of Dirac structures for the vector current is given in [19]. We choose a different basis for both vector and axialvector currents. We compile the list of all Dirac structures $\Gamma_{V(A),i}^{\alpha\mu}$ in appendix B.

We define the helicity amplitudes for the two currents $\Gamma^\mu = \gamma^\mu, \gamma^\mu\gamma_5$ as

$$\mathcal{A}_\Gamma(s_b, s_c, \lambda_c, \lambda_q) \equiv \langle \Lambda_c^*(s_c, \eta(\lambda_c))|\,\bar{c}\,\Gamma^\mu \varepsilon_\mu^*(\lambda_q) b\,|\Lambda_b(s_b)\rangle\,, \tag{2.4}$$

where the $\varepsilon_\mu^*(\lambda_q)$ are a basis of polarisation vectors for the virtual W exchange with the polarisation states $\lambda_q \in \{t, 0, +1, -1\}$; see appendix D. Due to the fact that the angular momentum configurations λ_c and s_c in eq. (2.4) can be independently chosen, there are

JHEP06(2018)155

more possible combinations of λ_c and s_c than physically permitted. We identify the helicity amplitudes with total angular moment $J = 1/2$ as

$$\begin{aligned}
\mathcal{A}_\Gamma^{(1/2)}(+1/2,+1/2,0) &\equiv -\sqrt{\frac{1}{3}}\mathcal{A}_\Gamma(+1/2,+1/2,0,0) + \sqrt{\frac{2}{3}}\mathcal{A}_\Gamma(+1/2,-1/2,+1,0)\,,\\
\mathcal{A}_\Gamma^{(1/2)}(+1/2,+1/2,t) &\equiv -\sqrt{\frac{1}{3}}\mathcal{A}_\Gamma(+1/2,+1/2,0,t) + \sqrt{\frac{2}{3}}\mathcal{A}_\Gamma(+1/2,-1/2,+1,t)\,,\\
\mathcal{A}_\Gamma^{(1/2)}(+1/2,-1/2,-1) &\equiv \sqrt{\frac{1}{3}}\mathcal{A}_\Gamma(+1/2,-1/2,0,-1) - \sqrt{\frac{2}{3}}\mathcal{A}_\Gamma(+1/2,+1/2,-1,-1)\,.
\end{aligned} \tag{2.5}$$

The complementary set of $J = 3/2$ amplitudes reads

$$\begin{aligned}
\mathcal{A}_\Gamma^{(3/2)}(+1/2,+3/2,+1) &\equiv \mathcal{A}_\Gamma(+1/2,+1/2,+1,+1)\,,\\
\mathcal{A}_\Gamma^{(3/2)}(+1/2,+1/2,0) &\equiv \sqrt{\frac{2}{3}}\mathcal{A}_\Gamma(+1/2,+1/2,0,0) + \sqrt{\frac{1}{3}}\mathcal{A}_\Gamma^{(3/2)}(+1/2,-1/2,+1,0)\,,\\
\mathcal{A}_\Gamma^{(3/2)}(+1/2,+1/2,t) &\equiv \sqrt{\frac{2}{3}}\mathcal{A}_\Gamma(+1/2,+1/2,0,t) + \sqrt{\frac{1}{3}}\mathcal{A}_\Gamma^{(3/2)}(+1/2,-1/2,+1,t)\,,\\
\mathcal{A}_\Gamma^{(3/2)}(+1/2,-1/2,-1) &\equiv \sqrt{\frac{2}{3}}\mathcal{A}_\Gamma(+1/2,-1/2,0,-1) + \sqrt{\frac{1}{3}}\mathcal{A}_\Gamma^{(3/2)}(+1/2,+1/2,-1,-1)\,.
\end{aligned} \tag{2.6}$$

For transitions to $J = 1/2$ the set of amplitudes in eq. (2.6) is required to vanish identically, and similarly for transitions to $J = 3/2$ the set in eq. (2.5) needs to be zero. We explicitly verify this to be the case for the structures listed in appendix B.

Our Dirac structures $\Gamma^{\alpha\mu}_{V(A),i}$ have been chosen such that the form factors $F_{1/2,\lambda_q}$ and $G_{1/2,\lambda_q}$, $\lambda_q \in \{t, 0, \perp\}$, correspond to transitions into $\Lambda_c(2595)^+$ states with $|J_z| = 1/2$, while the $\Lambda_c(2625)^+$ states with $|J_z| = 3/2$ are only produced via the form factors $F_{3/2,\perp}$ and $G_{3/2,\perp}$. Note that all helicity amplitudes depend only on one single form factor; see eqs. (C.31)–(C.33), eqs. (C.34)–(C.36), eqs. (C.73)–(C.76), and eqs. (C.77)–(C.80). We have therefore achieved a decomposition of the (axial)vector hadronic matrix elements in terms of helicity form factors as inspired by [20]. We note that our definitions of the form factors differ from the one adopted in [18], where the decomposition of the vector and axial vector hadronic matrix elements do not yield form factors for transitions with well-defined angular momentum of the final states. In particular in the conventions of [18] the time-like polarisation, which is relevant for the LFU ratio $R_{\Lambda_c^*}$, depends on linear combinations of multiple form factors instead of one form factor per current.

2.2 Heavy-quark expansion

In ref. [18], the usual basis of form factors has been studied in the HQE up to $1/m$ contributions. We cross-check their results, and adapt them to our choice of a helicity basis for the form factors. In particular, we study the hadronic matrix elements in and beyond the heavy quark limit $m_b \to \infty$, $m_c \to \infty$ with $m_c/m_b = \text{const}$. Following [17], we use that the transition matrix elements can be written at leading power in the expansion as

$$\langle \Lambda_c^*(k,\eta,s_c)|\,\bar{c}\,\Gamma^\mu b\,|\Lambda_b^0(p,s_b)\rangle = \sqrt{4}\bar{u}_\alpha(m_{\Lambda_c^*}v',\eta,s_c)\Gamma^\mu u(m_{\Lambda_b}v,s_b)\zeta^\alpha(w)\,, \tag{2.7}$$

JHEP06(2018)155

where $w \equiv v \cdot v' = (m_{\Lambda_b}^2 + m_{\Lambda_c^*}^2 - q^2)/(2m_{\Lambda_b} m_{\Lambda_c^*})$, v and v' are the four-velocities of the initial and final states, respectively, and Γ denotes a Dirac structure. Here the most general decomposition of the light-state transition amplitude ζ reads

$$\zeta^\alpha(w) = \zeta(w)(v - v')^\alpha \,. \tag{2.8}$$

As a consequence, at leading power all form factors can be expressed in terms of the single amplitude $\zeta(w)$, which must vanish at the zero hadronic recoil $w = 1$, which corresponds to $q^2 = (m_{\Lambda_b} - m_{\Lambda_c^*})^2$. In order to include also $1/m$ and α_s corrections, we use for the vector current (and similarly for the axialvector current)

$$\gamma^\mu \mapsto J_V^\mu = C_1(\bar{w})\gamma^\mu + C_2(\bar{w})v^\mu + C_3(\bar{w})v'^\mu + \Delta J_V^\mu\big|_{\mathcal{O}_1} + \Delta J_V^\mu\big|_{\mathcal{O}_8} + \mathcal{O}(\alpha_s/m, 1/m^2)\,, \tag{2.9}$$

with perturbative coefficients C_i and power corrections ΔJ_V^μ.

The perturbative functions C_i are the Wilson coefficients arising in the matching of HQET onto QCD. Their argument $\bar{w}$ is the recoil parameter as experienced by the heavy quarks within the hadrons. Note that for a decay to orbitally excited hadrons $\bar{w}$ is not the same as defined for transitions among ground-state baryons. Instead, we use

$$\bar{w} \equiv w\left(1 + \frac{\bar{\Lambda}}{m_b} + \frac{\bar{\Lambda}'}{m_c}\right) - \left(\frac{\bar{\Lambda}}{m_c} + \frac{\bar{\Lambda}'}{m_b}\right)\,, \tag{2.10}$$

where $\bar{\Lambda}$ and $\bar{\Lambda}'$ are the usual HQET parameters in the infinite mass limit. In the following we choose to use the pole mass scheme to determine the $\Lambda^{(\prime)}$ parameters from the respective baryon masses. Our eq. (2.10) yields the product of heavy-quark velocities as defined in [21] in the limit $\bar{\Lambda}' \to \bar{\Lambda}$. We use the matching coefficients C_i to order α_s, which are given in eq. (3.111) of [21]. At the precision that we aim for, we do not require the renormalization-group improved matching coefficients, which can be extracted from [21], eq. (3.121).

In eq. (2.9) we use only power corrections $\Delta J_V^\mu\big|_{\mathcal{O}_1}$ and $\Delta J_V^\mu\big|_{\mathcal{O}_8}$, arising from the local operators $\mathcal{O}_1$ and $\mathcal{O}_8$ as defined in [21], respectively. The remaining local operators only contribute at the order α_s/m and are therefore beyond the precision we aim for. The hadronic matrix elements of $\mathcal{O}_1$ and $\mathcal{O}_8$ can be parametrised as:

$$\langle \Lambda_c^*(k,\eta,s_c)|\,\Delta J_{V\mu}\big|_{\mathcal{O}_{1(8)}}\,|\Lambda_b^0(p,s_b)\rangle = \sqrt{4}\bar{u}_\alpha(m_{\Lambda_c^*}v',\eta,s_c)\big[\mathcal{O}_{1(8)}\big]_{\mu\beta}u(m_{\Lambda_b}v,s_b)\zeta_{b(c)}^{\alpha\beta}(w)\,, \tag{2.11}$$

where

$$\zeta_{(q)}^{\alpha\beta}(w) = (v - v')^\alpha\left[\zeta_1^{(q)}(w)v^\beta + \zeta_2^{(q)}(w)v'^\beta\right] + g^{\alpha\beta}\zeta_3^{(q)}(w)\,, \tag{2.12}$$

and $[\mathcal{O}_1]_{\mu\beta} = \gamma_\mu\gamma_\beta$, $[\mathcal{O}_8]_{\mu\beta} = \gamma_\beta\gamma_\mu$.

JHEP06(2018)155

After some algebra, we obtain the following for the contributions from $\Delta J_{V\mu}\big|_{\mathcal{O}_1}$ and $\Delta J_{V\mu}\big|_{\mathcal{O}_8}$:

$$\begin{aligned}
\langle\Lambda_c^*(k,\eta,s_c)|\,\Delta J_{V\mu}\big|_{\mathcal{O}_1}\,|\Lambda_b^0(p,s_b)\rangle &= \frac{1}{2m_b}\Big[2\bar{u}_\alpha(m_{\Lambda_c^*}v',\eta,s_c)\gamma_\mu u(m_{\Lambda_b}v,s_b)v^\alpha\left(\zeta_1^{(b)}(w)-\zeta_2^{(b)}(w)\right)\\
&\quad+4\bar{u}_\alpha(m_{\Lambda_c^*}v',\eta,s_c)u(m_{\Lambda_b}v,s_b)v^\alpha v'^\mu\zeta_2^{(b)}(w)\\
&\quad+2\bar{u}_\alpha(m_{\Lambda_c^*}v',\eta,s_c)\gamma_\mu\gamma^\alpha u(m_{\Lambda_b}v,s_b)\zeta_3^{(b)}(w)\Big]\,,\\
\langle\Lambda_c^*(k,\eta,s_c)|\,\Delta J_{V\mu}\big|_{\mathcal{O}_8}\,|\Lambda_b^0(p,s_b)\rangle &= \frac{1}{2m_c}\Big[2\bar{u}_\alpha(m_{\Lambda_c^*}v',\eta,s_c)\gamma_\mu u(m_{\Lambda_b}v,s_b)v^\alpha\left(\zeta_2^{(c)}(w)-\zeta_1^{(c)}(w)\right)\\
&\quad+4\bar{u}_\alpha(m_{\Lambda_c^*}v',\eta,s_c)u(m_{\Lambda_b}v,s_b)v^\alpha v^\mu\zeta_1^{(c)}(w)\\
&\quad+2\bar{u}_\alpha(m_{\Lambda_c^*}v',\eta,s_c)\gamma^\alpha\gamma_\mu u(m_{\Lambda_b}v,s_b)\zeta_3^{(c)}(w)\Big]\,.
\end{aligned}\tag{2.13}$$

We can follow the very same steps also with the axial vector current. In this case we have:

$$\begin{aligned}
\gamma^\mu\gamma_5 \mapsto J_A^\mu &= C_1^{(5)}(\bar{w})\gamma^\mu\gamma^5 + C_2^{(5)}(\bar{w})v^\mu\gamma^5 + C_3^{(5)}(\bar{w})v'^\mu\gamma^5\\
&\quad+\Delta J_A^\mu\big|_{\mathcal{O}_1^A}+\Delta J_A^\mu\big|_{\mathcal{O}_8^A}+\mathcal{O}(\alpha_s/m,1/m^2)\,,
\end{aligned}\tag{2.14}$$

where the subleading contributions $\Delta J_A^\mu\big|_{\mathcal{O}_1^A}$ and $\Delta J_A^\mu\big|_{\mathcal{O}_8^A}$ can by computed from

$$\langle\Lambda_c^*(k,\eta,s_c)|\,\Delta J_{A\mu}\big|_{\mathcal{O}^A_{1(8)}}\,|\Lambda_b^0(p,s_b)\rangle = \sqrt{4}\bar{u}_\alpha(m_{\Lambda_c^*}v',\eta,s_c)[\mathcal{O}^A_{1(8)}]_{\mu\beta}u(m_{\Lambda_b}v,s_b)\zeta^{\alpha\beta}_{b(c)}(w)\,,\tag{2.15}$$

and $[\mathcal{O}_1^A]_{\mu\beta}=\gamma_\mu\gamma^5\gamma_\beta$, $[\mathcal{O}_8^A]_{\mu\beta}=\gamma_\beta\gamma_\mu\gamma^5$. From this we obtain:

$$\begin{aligned}
\langle\Lambda_c^*(k,\eta,s_c)|\,\Delta J_{A\mu}\big|_{\mathcal{O}_1^A}\,|\Lambda_b^0(p,s_b)\rangle &= \frac{1}{2m_b}\Big[2\bar{u}_\alpha(m_{\Lambda_c^*}v',\eta,s_c)\gamma_\mu u(m_{\Lambda_b}v,s_b)v^\alpha\left(\zeta_1^{(b)}(w)+\zeta_2^{(b)}(w)\right)\\
&\quad-4\bar{u}_\alpha(m_{\Lambda_c^*}v',\eta,s_c)u(m_{\Lambda_b}v,s_b)v^\alpha v'^\mu\zeta_2^{(b)}(w)\\
&\quad+2\bar{u}_\alpha(m_{\Lambda_c^*}v',\eta,s_c)\gamma^\mu\gamma^5\gamma^\alpha u(m_{\Lambda_b}v,s_b)\zeta_3^{(b)}(w)\Big]\,,\\
\langle\Lambda_c^*(k,\eta,s_c)|\,\Delta J_{A\mu}\big|_{\mathcal{O}_8^A}\,|\Lambda_b^0(p,s_b)\rangle &= \frac{1}{2m_c}\Big[2\bar{u}_\alpha(m_{\Lambda_c^*}v',\eta,s_c)\gamma_\mu u(m_{\Lambda_b}v,s_b)v^\alpha\left(\zeta_1^{(c)}(w)+\zeta_2^{(c)}(w)\right)\\
&\quad+4\bar{u}_\alpha(m_{\Lambda_c^*}v',\eta,s_c)u(m_{\Lambda_b}v,s_b)v^\alpha v^\mu\zeta_1^{(c)}(w)\\
&\quad+2\bar{u}_\alpha(m_{\Lambda_c^*}v',\eta,s_c)\gamma^\alpha\gamma^\mu\gamma^5 u(m_{\Lambda_b}v,s_b)\zeta_3^{(c)}(w)\Big]\,.
\end{aligned}\tag{2.16}$$

The subleading IW functions are related by the equations of motion. In particular we have that $v_\beta\zeta^{\alpha\beta}_{(b)}=0$, and $v'_\beta\zeta^{\alpha\beta}_{(c)}=0$. This leads to the following relations:

$$\zeta_1^{(b)}(w)+w\zeta_2^{(b)}(w)+\zeta_3^{(b)}(w)=0\,,\tag{2.17}$$

$$w\zeta_1^{(c)}(w)+\zeta_2^{(c)}(w)=0\,.\tag{2.18}$$

JHEP06(2018)155

Furthermore we know that $i\partial_\alpha[\bar{h}_c(v')\Gamma h_b(v)] = \bar{h}_c(v')i\overleftarrow{D}_\alpha\Gamma h_b(v) + \bar{h}_c(v')\Gamma i D_\alpha h_b(v)$, where we denote $h_{b(c)}$ as the usual HQET fields. This identity allows us to write the following relations:

$$\zeta_1^{(b)}(w) + \zeta_1^{(c)}(w) = \bar{\Lambda}\zeta(w)\,, \tag{2.19}$$

$$\zeta_2^{(b)}(w) + \zeta_2^{(c)}(w) = -\bar{\Lambda}'\zeta(w)\,, \tag{2.20}$$

$$\zeta_3^{(b)}(w) + \zeta_3^{(c)}(w) = 0\,. \tag{2.21}$$

With these 5 relations we can reduce the initial 6 subleading IW functions to one independent subleading IW function. We find it convenient to use $\zeta_3^{(b)}$:

$$\begin{aligned}
\zeta_1^{(b)} &= -\frac{\zeta_3^{(b)}}{1-w^2} + \frac{w\zeta}{1-w^2}\left(\bar{\Lambda}' - \bar{\Lambda}w\right)\,, \qquad \zeta_2^{(b)} = +\frac{w\zeta_3^{(b)}}{1-w^2} - \frac{\zeta}{1-w^2}\left(\bar{\Lambda}' - \bar{\Lambda}w\right)\,, \\
\zeta_1^{(c)} &= +\frac{\zeta_3^{(b)}}{1-w^2} - \frac{\zeta}{1-w^2}\left(w\bar{\Lambda}' - \bar{\Lambda}\right)\,, \qquad \zeta_2^{(c)} = -\frac{w\zeta_3^{(b)}}{1-w^2} + \frac{w\zeta}{1-w^2}\left(w\bar{\Lambda}' - \bar{\Lambda}\right)\,.
\end{aligned} \tag{2.22}$$

From this point on we identify $\zeta_{\rm SL} \equiv \zeta_3^{(b)} = -\zeta_3^{(c)}$.

Beside the effects on local operators, we also need to consider effects from non-local insertions of the HQET Lagrangian at power $1/m$. Following the discussion in [18, 21], non-local insertions of the kinetic operator give rise to an w-dependent shift $\eta_{\rm kin}(w)$ to the leading-power IW function $\zeta(w)$. We can absorb this shift into the definition of ζ:

$$\zeta(w) + \frac{1}{2m_b m_c}\left[m_b + m_c\right]\eta_{\rm kin}(w) \mapsto \zeta(w)\,. \tag{2.23}$$

The w-dependent shift due to the chromomagnetic operator is more delicate. The two contributions are:

$$\eta_{\rm mag}^{(c)}(w) : \left[g_{\mu\alpha}v_\nu\right]\bar{u}_J^\alpha(m_{\Lambda_c^*}v', \eta, s_c)\; i\sigma^{\mu\nu}\frac{1+\not{v}'}{2}\Gamma u(m_{\Lambda_b}v, s_b) \tag{2.24}$$

$$\eta_{\rm mag}^{(b)}(w) : \left[g_{\mu\alpha}v'_\nu\right]\bar{u}_J^\alpha(m_{\Lambda_c^*}v', \eta, s_c)\;\Gamma\frac{1+\not{v}}{2}\; i\sigma^{\mu\nu}u(m_{\Lambda_b}v, s_b)\,. \tag{2.25}$$

In [18], it is argued that the two functions $\eta_{\rm mag}^{(q)}(w)$ must vanish at zero recoil, and are expected to be small compared to the size of $\Lambda_{\rm QCD}$. We follow this argument, and therefore choose to not consider contributions from either $\eta_{\rm mag}^{(q)}(w)$ from this point on.

If we want now to express the form factors in terms of the leading and subleading IW functions we need to match the HQE expansion of the helicity amplitudes onto the direct calculation presented in section 2.1. Concerning the $\Lambda_c(2595)^+$ final state, the comparison

JHEP06(2018)155

between eqs. (C.37)–(C.39) and eqs. (C.31)–(C.33) leads to

$$f_{1/2,0} = \frac{\sqrt{s_+}}{2(m_{\Lambda_b} m_{\Lambda_c^*})^{3/2}} \Bigg\{ \Bigg[s_- \left(C_1(\bar{w}) + \frac{s_+ (C_2(\bar{w}) m_{\Lambda_c^*} + C_3(\bar{w}) m_{\Lambda_b})}{2 m_{\Lambda_b} m_{\Lambda_c^*} (m_{\Lambda_b} + m_{\Lambda_c^*})} \right) + \frac{(m_{\Lambda_b} - m_{\Lambda_c^*})}{m_{\Lambda_b} + m_{\Lambda_c^*}} \left(\frac{m_{\Lambda_b}^2 - m_{\Lambda_c^*}^2 + q^2}{2 m_{\Lambda_b}} \bar{\Lambda} - \frac{m_{\Lambda_b}^2 - m_{\Lambda_c^*}^2 - q^2}{2 m_{\Lambda_c^*}} \bar{\Lambda}' \right) \Bigg] \zeta - 2 (m_{\Lambda_b} - m_{\Lambda_c^*}) \zeta_{\rm SL} \Bigg\}, \tag{2.26}$$

$$f_{1/2,t} = \frac{\sqrt{s_-}}{2(m_{\Lambda_b} m_{\Lambda_c^*})^{3/2}} \Bigg\{ \Bigg[C_1(\bar{w}) s_+ + \frac{m_{\Lambda_b} + m_{\Lambda_c^*}}{m_{\Lambda_b} - m_{\Lambda_c^*}} \left(\frac{m_{\Lambda_b}^2 - m_{\Lambda_c^*}^2 + q^2}{2 m_{\Lambda_b}} \left(\bar{\Lambda} + \frac{C_2(\bar{w}) s_+}{m_{\Lambda_b} + m_{\Lambda_c^*}} \right) - \frac{m_{\Lambda_b}^2 - m_{\Lambda_c^*}^2 - q^2}{2 m_{\Lambda_c^*}} \left(\bar{\Lambda}' - \frac{C_3(\bar{w}) s_+}{m_{\Lambda_b} + m_{\Lambda_c^*}} \right) \right) \Bigg] \zeta - 2 \frac{(m_{\Lambda_b} + m_{\Lambda_c^*})^2}{m_{\Lambda_b} - m_{\Lambda_c^*}} \zeta_{\rm SL} \Bigg\}, \tag{2.27}$$

$$f_{1/2,\perp} = \frac{\sqrt{s_+}}{2(m_{\Lambda_b} m_{\Lambda_c^*})^{3/2}} \Bigg\{ \Bigg[C_1(\bar{w}) s_- + \frac{3 m_{\Lambda_b}^2 + m_{\Lambda_c^*}^2 - q^2}{2 m_{\Lambda_b}} \bar{\Lambda} - \frac{m_{\Lambda_b}^2 + 3 m_{\Lambda_c^*}^2 - q^2}{2 m_{\Lambda_c^*}} \bar{\Lambda}' \Bigg] \zeta - 2 m_{\Lambda_b} \zeta_{\rm SL} \Bigg\}, \tag{2.28}$$

for the vector form factors, while for the axial-vector form factors the matching of eqs. (C.40)–(C.42) onto eqs. (C.34)–(C.36) gives

$$g_{1/2,0} = \frac{\sqrt{s_-}}{2(m_{\Lambda_b} m_{\Lambda_c^*})^{3/2}} \Bigg\{ \Bigg[s_+ \left(C_1(\bar{w}) - \frac{s_- (C_2(\bar{w}) m_{\Lambda_c^*} + C_3(\bar{w}) m_{\Lambda_b})}{2 m_{\Lambda_b} m_{\Lambda_c^*} (m_{\Lambda_b} - m_{\Lambda_c^*})} \right) + \frac{m_{\Lambda_b} + m_{\Lambda_c^*}}{m_{\Lambda_b} - m_{\Lambda_c^*}} \left(\frac{m_{\Lambda_b}^2 - m_{\Lambda_c^*}^2 + q^2}{2 m_{\Lambda_b}} \bar{\Lambda} - \frac{m_{\Lambda_b}^2 - m_{\Lambda_c^*}^2 - q^2}{2 m_{\Lambda_c^*}} \bar{\Lambda}' \right) \Bigg] \zeta - 2 (m_{\Lambda_b} + m_{\Lambda_c^*}) \zeta_{\rm SL} \Bigg\}, \tag{2.29}$$

$$g_{1/2,t} = \frac{\sqrt{s_+}}{2(m_{\Lambda_b} m_{\Lambda_c^*})^{3/2}} \Bigg\{ \Bigg[C_1(\bar{w}) s_- + \frac{m_{\Lambda_b} - m_{\Lambda_c^*}}{m_{\Lambda_b} + m_{\Lambda_c^*}} \left(\frac{m_{\Lambda_b}^2 - m_{\Lambda_c^*}^2 + q^2}{2 m_{\Lambda_b}} \left(\bar{\Lambda} - \frac{C_2(\bar{w}) s_-}{m_{\Lambda_b} - m_{\Lambda_c^*}} \right) - \frac{m_{\Lambda_b}^2 - m_{\Lambda_c^*}^2 - q^2}{2 m_{\Lambda_c^*}} \left(\bar{\Lambda}' + \frac{C_3(\bar{w}) s_-}{m_{\Lambda_b} - m_{\Lambda_c^*}} \right) \right) \Bigg] \zeta - 2 \frac{(m_{\Lambda_b} - m_{\Lambda_c^*})^2}{m_{\Lambda_b} + m_{\Lambda_c^*}} \zeta_{\rm SL} \Bigg\}, \tag{2.30}$$

$$g_{1/2,\perp} = \frac{\sqrt{s_-}}{2(m_{\Lambda_b} m_{\Lambda_c^*})^{3/2}} \Bigg\{ \Bigg[C_1(\bar{w}) s_+ + \bar{\Lambda} \frac{3 m_{\Lambda_b}^2 + m_{\Lambda_c^*}^2 - q^2}{2 m_{\Lambda_b}} - \bar{\Lambda}' \frac{m_{\Lambda_b}^2 + 3 m_{\Lambda_c^*}^2 - q^2}{2 m_{\Lambda_c^*}} \Bigg] \zeta - 2 m_{\Lambda_b} \zeta_{\rm SL} \Bigg\}. \tag{2.31}$$

Here and in the following we denote $s_\pm \equiv (m_{\Lambda_b} \pm m_{\Lambda_c^*})^2 - q^2$. Concerning the $\Lambda_c(2625)^+$ final state, the vector form factors are obtained by matching eqs. (C.81)–(C.84) with

JHEP06(2018)155

eqs. (C.73)–(C.76)

$$F_{1/2,\perp} = \frac{\sqrt{s_+}}{2(m_{\Lambda_b} m_{\Lambda_c^*})^{3/2}} \left\{ \left[C_1(\bar{w}) s_- + \frac{3m_{\Lambda_b}^2 + m_{\Lambda_c^*}^2 - q^2}{2m_{\Lambda_b}} \bar{\Lambda} - \frac{m_{\Lambda_b}^2 + 3m_{\Lambda_c^*}^2 - q^2}{2m_{\Lambda_c^*}} \bar{\Lambda}' \right] \zeta + m_{\Lambda_b} \zeta_{\rm SL} \right\}, \tag{2.32}$$

$$\begin{aligned} F_{1/2,t} = \frac{\sqrt{s_-}}{2(m_{\Lambda_b} m_{\Lambda_c^*})^{3/2}} \Bigg\{ \Bigg[& C_1(\bar{w}) s_+ + \frac{m_{\Lambda_b} + m_{\Lambda_c^*}}{m_{\Lambda_b} - m_{\Lambda_c^*}} \left(\frac{m_{\Lambda_b}^2 - m_{\Lambda_c^*}^2 + q^2}{2m_{\Lambda_b}} \left(\bar{\Lambda} + \frac{C_2(\bar{w}) s_+}{m_{\Lambda_b} + m_{\Lambda_c^*}} \right) \right. \\ & \left. - \frac{m_{\Lambda_b}^2 - m_{\Lambda_c^*}^2 - q^2}{2m_{\Lambda_c^*}} \left(\bar{\Lambda}' - \frac{C_3(\bar{w}) s_+}{m_{\Lambda_b} + m_{\Lambda_c^*}} \right) \right) \Bigg] \zeta + \frac{(m_{\Lambda_b} + m_{\Lambda_c^*})^2}{m_{\Lambda_b} - m_{\Lambda_c^*}} \zeta_{\rm SL} \Bigg\}, \end{aligned} \tag{2.33}$$

$$\begin{aligned} F_{1/2,0} = \frac{\sqrt{s_+}}{2(m_{\Lambda_b} m_{\Lambda_c^*})^{3/2}} \Bigg\{ \Bigg[& s_- \left(C_1(\bar{w}) + \frac{s_+ (C_2(\bar{w}) m_{\Lambda_c^*} + C_3(\bar{w}) m_{\Lambda_b})}{2m_{\Lambda_b} m_{\Lambda_c^*} (m_{\Lambda_b} + m_{\Lambda_c^*})} \right) \\ & + \frac{m_{\Lambda_b} - m_{\Lambda_c^*}}{m_{\Lambda_b} + m_{\Lambda_c^*}} \left(\frac{m_{\Lambda_b}^2 - m_{\Lambda_c^*}^2 + q^2}{2m_{\Lambda_b}} \bar{\Lambda} - \frac{m_{\Lambda_b}^2 - m_{\Lambda_c^*}^2 - q^2}{2m_{\Lambda_c^*}} \bar{\Lambda}' \right) \Bigg] \zeta + (m_{\Lambda_b} - m_{\Lambda_c^*}) \zeta_{\rm SL} \Bigg\}, \end{aligned} \tag{2.34}$$

$$F_{3/2,\perp} = -\frac{\sqrt{s_+}}{2m_{\Lambda_b}^{3/2} m_{\Lambda_c^*}^{1/2}} \zeta_{\rm SL}\,, \tag{2.35}$$

while for the axial-vector form factor the comparison of eqs. (C.85)–(C.88) and eqs. (C.77)–(C.80) yields

$$G_{1/2,\perp} = \frac{\sqrt{s_-}}{2(m_{\Lambda_b} m_{\Lambda_c^*})^{3/2}} \left\{ \left[C_1(\bar{w}) s_+ + \frac{3m_{\Lambda_b}^2 + m_{\Lambda_c^*}^2 - q^2}{2m_{\Lambda_b}} \bar{\Lambda} - \frac{m_{\Lambda_b}^2 + 3m_{\Lambda_c^*}^2 - q^2}{2m_{\Lambda_c^*}} \bar{\Lambda}' \right] \zeta + m_{\Lambda_b} \zeta_{\rm SL} \right\}, \tag{2.36}$$

$$\begin{aligned} G_{1/2,t} = \frac{\sqrt{s_+}}{2(m_{\Lambda_b} m_{\Lambda_c^*})^{3/2}} \Bigg\{ \Bigg[& C_1(\bar{w}) s_- + \frac{m_{\Lambda_b} - m_{\Lambda_c^*}}{m_{\Lambda_b} + m_{\Lambda_c^*}} \left(\frac{m_{\Lambda_b}^2 - m_{\Lambda_c^*}^2 + q^2}{2m_{\Lambda_b}} \left(\bar{\Lambda} - \frac{C_2(\bar{w}) s_-}{m_{\Lambda_b} - m_{\Lambda_c^*}} \right) \right. \\ & \left. - \frac{m_{\Lambda_b}^2 - m_{\Lambda_c^*}^2 - q^2}{2m_{\Lambda_c^*}} \left(\bar{\Lambda}' + \frac{C_3(\bar{w}) s_-}{m_{\Lambda_b} - m_{\Lambda_c^*}} \right) \right) \Bigg] \zeta + \frac{(m_{\Lambda_b} - m_{\Lambda_c^*})^2}{m_{\Lambda_b} + m_{\Lambda_c^*}} \zeta_{\rm SL} \Bigg\}, \end{aligned} \tag{2.37}$$

$$\begin{aligned} G_{1/2,0} = \frac{\sqrt{s_-}}{2(m_{\Lambda_b} m_{\Lambda_c^*})^{3/2}} \Bigg\{ \Bigg[& s_+ \left(C_1(\bar{w}) - \frac{s_- (C_2(\bar{w}) m_{\Lambda_c^*} + C_3(\bar{w}) m_{\Lambda_b})}{2m_{\Lambda_b} m_{\Lambda_c^*} (m_{\Lambda_b} - m_{\Lambda_c^*})} \right) \\ & + \frac{m_{\Lambda_b} + m_{\Lambda_c^*}}{m_{\Lambda_b} - m_{\Lambda_c^*}} \left(\frac{m_{\Lambda_b}^2 - m_{\Lambda_c^*}^2 + q^2}{2m_{\Lambda_b}} \bar{\Lambda} - \frac{m_{\Lambda_b}^2 - m_{\Lambda_c^*}^2 - q^2}{2m_{\Lambda_c^*}} \bar{\Lambda}' \right) \Bigg] \zeta + (m_{\Lambda_b} + m_{\Lambda_c^*}) \zeta_{\rm SL} \Bigg\}, \end{aligned} \tag{2.38}$$

$$G_{3/2,\perp} = -\frac{\sqrt{s_-}}{2m_{\Lambda_b}^{3/2} m_{\Lambda_c^*}^{1/2}} \zeta_{\rm SL}\,. \tag{2.39}$$

Thus, at leading power in $1/m$ only the $(J, J_z) = (3/2, \pm 1/2)$ form factors receive contributions from the leading-power IW function. As a consequence, the sum rule at zero recoil ($w = 1$ or $s_- = 0$) as discussed later will be less sensitive to the contributions from the $J = 3/2$ amplitudes.

JHEP06(2018)155

We note in passing that our results for the HQE of the form factors fulfil the relations

$$\begin{aligned} \frac{f_{1/2,t}(0)}{f_{1/2,0}(0)} &\equiv \frac{m_{\Lambda_b}+m_{\Lambda_c^*}}{m_{\Lambda_b}-m_{\Lambda_c^*}}\,, \quad \frac{g_{1/2,t}(0)}{g_{1/2,0}(0)} \equiv \frac{m_{\Lambda_b}-m_{\Lambda_c^*}}{m_{\Lambda_b}+m_{\Lambda_c^*}}\,, \\ \frac{F_{1/2,t}(0)}{F_{1/2,0}(0)} &\equiv \frac{m_{\Lambda_b}+m_{\Lambda_c^*}}{m_{\Lambda_b}-m_{\Lambda_c^*}}\,, \quad \frac{G_{1/2,t}(0)}{G_{1/2,0}(0)} \equiv \frac{m_{\Lambda_b}-m_{\Lambda_c^*}}{m_{\Lambda_b}+m_{\Lambda_c^*}}\,, \end{aligned} \tag{2.40}$$

as required by analyticity; i.e., any spurious poles of the hadronic matrix elements in the limit $q^2 \to 0$ do not correspond to any physical states with quantum numbers $B = -C = 1$, and therefore must be cancelled due to the above relations.

3 Phenomenology

3.1 Parametrisation of the Isgur-Wise functions

Determining the parameters of the leading and subleading IW functions is a crucial point to evaluate the form factors. Unfortunately, there are no first principles in HQET which allow us to estimate the q^2 dependence of the IW functions. In light of this, we need to infer a functional form for $\zeta(q^2)$ and $\zeta_{\rm SL}(q^2)$ through some other means. For the ground-state transition $\Lambda_b \to \Lambda_c$ and in the large N_c limit, it has been motivated in [22] to express the IW functions as exponential functions. Inspired by this, one of the models we consider here for the parametrisation of the leading and subleading IW function $\zeta(q^2)$ and $\zeta_{\rm SL}(q^2)$ is

$$\begin{aligned} \zeta(q^2)\Big|_{\rm exp} &\equiv \zeta(q^2_{\rm max}) \exp\left[\rho\left(\frac{q^2}{q^2_{\rm max}}-1\right)\right], \\ \zeta_{\rm SL}(q^2)\Big|_{\rm exp} &\equiv \zeta(q^2_{\rm max})\delta_{\rm SL} \exp\left[\frac{\rho_{\rm SL}}{\delta_{\rm SL}}\left(\frac{q^2}{q^2_{\rm max}}-1\right)\right], \end{aligned} \tag{3.1}$$

where the normalisation $\zeta(q^2_{\rm max})$, the relative normalisation $\delta_{\rm SL}$ and the two shape parameters ρ and $\rho_{\rm SL}$ are to be determined.

We can also use a Taylor expansion of $\zeta(q^2)$ and $\zeta_{\rm SL}(q^2)$ around $q^2 \simeq q^2_{\rm max}$. For our purposes we use an expansion up to the first order in q^2:

$$\begin{aligned} \zeta(q^2)\Big|_{\rm lin} &\equiv \zeta(q^2_{\rm max}) \left[1+\rho\left(\frac{q^2}{q^2_{\rm max}}-1\right)\right], \\ \zeta_{\rm SL}(q^2)\Big|_{\rm lin} &\equiv \zeta(q^2_{\rm max}) \left[\delta_{\rm SL}+\rho_{\rm SL}\left(\frac{q^2}{q^2_{\rm max}}-1\right)\right]. \end{aligned} \tag{3.2}$$

In the following we will refer to eq. (3.2) as the nominal parametrisation.

Both parametrisations have been chosen such that they share their complete parameter set, and such that both the leading and the subleading IW functions have a common normalisation $\zeta(q^2_{\rm max})$.

3.2 Benchmarking the form factors' parameters from Zero Recoil Sum Rules

The kinematic point of zero hadronic recoil is a special one for bottom-to-charm transitions. In this point the hadronic form factors for $\Lambda_b \to X_c$ transitions, where X_c denotes a

JHEP06(2018)155

singly-charmed baryonic state, are minimally sensitive to the dynamics of the light degrees of freedom within the respective hadrons; see e.g. [23]. As a consequence, the inclusive spectral density for the forward matrix elements of two bi-local insertions of the weak current can be expressed in terms of $\Lambda_b \to X_c$ form factors. Inference of weighted sum of squares for the form factor normalisations follows in what is known as a Zero Recoil Sum Rule (ZRSR) [24, 25]. This is only possible since the spectral density consists of a sum of positive-definite exclusive terms.

The ZRSR is well established for $B \to D$ and $B \to D^*$ transitions, with OPE contributions known up to order α_s^2 [26]. After the first lattice QCD results for the $\Lambda_b \to \Lambda_c$ form factors appeared [14], they were scrutinised in the ZRSR framework [27]. The conclusion of the latter analysis is as follows. Given our present knowledge of the Λ_b forward matrix elements, and given the lack of mixed α_s/m results for the ZRSR, the lattice results for $\Lambda_b \to \Lambda_c$ transition lead to a negative contribution from non-ground state transitions. As mentioned above, negative contributions to the spectral density are not possible by construction. Hence, either the inclusive calculation of the spectral density yields too small a value, or the lattice results are too large.

For the discussion at hand, we will assume that the inclusive calculation underestimates the magnitude of the spectral density. Specifically, we assume that $1/m^4$ and $1/m^5$ terms in the Heavy-Quark-Expansion, which have not been taken into account due to lack of information on the relevant hadronic matrix elements, will increase the magnitude. A priori it is not intuitive that terms at order $1/m^4$ or beyond can make a qualitative difference to the ZRSR. However, there is precedent for numerically relevant shifts in the case of $B \to D^*$ [28]. In the latter study, it was observed that — based on rather precise knowledge of the HQE parameters for B mesons — the sum of $1/m^4$ and $1/m^5$ terms yields roughly a third of the $1/m^2$ and $1/m^3$ terms.

In the absence of further information on the Λ_b forward matrix elements, we will therefore proceed as follows. We will rescale the estimate of the $1/m^2$ and $1/m^3$ terms by a factor of 1.33, thereby copying the situation in $B \to D^*$ decays.[1] The corresponding shift can now accommodate fully the lattice results for the $\Lambda_b \to \Lambda_c$ form factors, as well as form factors for Λ_b decays to excited charm baryons. The setup of the ZRSR involves an upper bound on the excitation energies $\varepsilon \equiv M_{X_c} - M_{\Lambda_c}$ of the contributing charm baryons. For the analysis at hand, $\varepsilon \leq 0.7\,\text{GeV}$. Based on the known spectrum of charmed baryons [29, Ch. 109 Charmed Baryons], the ZRSR covers — beside the ground state — form factors for Λ_b decays into $\Sigma_c(2455)$, $\Sigma_c(2520)$, $\Lambda_c(2595)$, $\Lambda_c(2625)$, and $\Sigma_c(2800)$.[2] The Σ_c states form an isospin triplet and therefore carry isospin $I = 1$. Consequently, the

[1] We stress that this rescaling, and the corresponding shift to the inclusive upper bound on the form factor normalisations, is based on a supposition rather than data, and will only be used for the purpose of benchmarking the experimental sensitivity. Ultimately, only improved knowledge of the hadronic matrix elements will settle the discrepancy between the ZRSR and lattice results.

[2] We do not consider here the states of roughly 2.8 GeV to 2.9 GeV for which there exists no definite assignment as either a Λ_c, or a Σ_c state, or as a kinematical artifact in the $\Lambda_c\pi\pi$ spectrum. A recent LHCb analysis of $\Lambda_b \to \Lambda_c \ell\nu$ [16] suggests that the yield of $\Lambda_c\pi\pi$ background stemming from this kinematic region corresponds to roughly 10% of the first orbitally excited Λ_c^* states. Given the overall accuracy of our analysis, this further supports our decision not to consider these states.

JHEP06(2018)155

transitions $\Lambda_b \to \Sigma_c$ violate isospin conservation, and we will assume them to be further suppressed with respect to the $\Lambda_b \to \Lambda_c^*$ transitions. This supposition is corroborated by the non-observation of $\Lambda_b \to \Sigma_c \ell\nu$ decays in the recent LHCb study [16]. Under the above assumptions, the inelastic parts of the ZRSR can be recast as matrix elements involving only $\Lambda_b \to \Lambda_c^*$ transitions.

Following the definitions and analysis of ref. [27], applying the assumptions above we arrive at the following constraints at zero recoil:

$$\begin{aligned} F_{\text{inel}} &= 0.011^{+0.061}_{-0.055} \approx F_{\text{inel},1/2} + F_{\text{inel},3/2}\,, \\ G_{\text{inel}} &= 0.040^{+0.049}_{-0.052} \approx G_{\text{inel},1/2} + G_{\text{inel},3/2}\,. \end{aligned} \tag{3.3}$$

The individual contributions from the orbitally-excited Λ_c^* states for the vector current read:

$$F_{\text{inel},1/2} \equiv \frac{1}{N_V} \sum_{\Lambda_c^* \text{ spin}} \langle \Lambda_b^0(v,s_b)|\, \bar{b}\gamma^\mu c\, |\Lambda_c(2595)^+(v)\rangle \langle \Lambda_c(2595)^+(v)|\, \bar{c}\gamma_\mu b\, |\Lambda_b^0(v,s_b)\rangle \tag{3.4}$$

$$= \frac{1}{3}\left[|f_{t,1/2}|^2 + |f_{0,1/2}|^2 \frac{(m_{\Lambda_b} + m_{\Lambda_c^*})^2}{(m_{\Lambda_b} - m_{\Lambda_c^*})^2} + 2|f_{\perp,1/2}|^2 \right]_{\text{zero recoil}}, \tag{3.5}$$

and

$$F_{\text{inel},3/2} \equiv \frac{1}{N_V} \sum_{\Lambda_c^* \text{ spin}} \langle \Lambda_b^0(v,s_b)|\, \bar{b}\gamma^\mu c\, |\Lambda_c(2625)^+(v)\rangle \langle \Lambda_c(2625)^+(v)|\, \bar{c}\gamma_\mu b\, |\Lambda_b^0(v,s_b)\rangle \tag{3.6}$$

$$= \frac{2}{3}\left[|F_{t,1/2}|^2 + |F_{0,1/2}|^2 \frac{(m_{\Lambda_b} + m_{\Lambda_c^*})^2}{(m_{\Lambda_b} - m_{\Lambda_c^*})^2} + 2|F_{\perp,1/2}|^2 + 6|F_{\perp,3/2}|^2 \right], \tag{3.7}$$

where $N_V = 1$. For the axialvector current, including the normalisation factor $N_A = 3$, the individual contributions read:

$$G_{\text{inel},1/2} \equiv \frac{1}{N_A} \sum_{\Lambda_c^* \text{ spin}} \langle \Lambda_b^0(v,s_b)|\, \bar{b}\gamma^\mu\gamma_5 c\, |\Lambda_c(2595)^+(v)\rangle \langle \Lambda_c(2595)^+(v)|\, \bar{c}\gamma_\mu\gamma_5 b\, |\Lambda_b^0(v,s_b)\rangle \tag{3.8}$$

$$= \frac{1}{9}\left[|g_{0,1/2}|^2 + |g_{t,1/2}|^2 \frac{(m_{\Lambda_b} + m_{\Lambda_c^*})^2}{(m_{\Lambda_b} - m_{\Lambda_c^*})^2} + 2|g_{\perp,1/2}|^2 \right]_{\text{zero recoil}}, \tag{3.9}$$

and

$$G_{\text{inel},1/2} \equiv \frac{1}{N_V} \sum_{\Lambda_c^* \text{ spin}} \langle \Lambda_b^0(v,s_b)|\, \bar{b}\gamma^\mu\gamma_5 c\, |\Lambda_c(2625)^+(v)\rangle \langle \Lambda_c(2625)^+(v)|\, \bar{c}\gamma_\mu\gamma_5 b\, |\Lambda_b^0(p,s_b)\rangle \tag{3.10}$$

$$= \frac{2}{9}\left[|G_{0,1/2}|^2 + |G_{t,1/2}|^2 \frac{(m_{\Lambda_b} + m_{\Lambda_c^*})^2}{(m_{\Lambda_b} - m_{\Lambda_c^*})^2} + 2|G_{\perp,1/2}|^2 + 6|G_{\perp,3/2}|^2 \right]_{\text{zero recoil}}. \tag{3.11}$$

In the zero-recoil point, both parametrisation eq. (3.1) and eq. (3.2) yield the same expressions, involving only the parameters $\zeta(q^2_{\text{max}})$ and δ_{SL}.

JHEP06(2018)155

Using two uncorrelated gaussian distributions for F_{inel} and G_{inel} and using symmetrised 68% intervals based on eq. (3.3) we obtain correlated distributions for $\zeta(q^2_{\text{max}})$ and δ_{SL}. The $\zeta(q^2_{\text{max}})$ distribution is highly non-gaussian, and due to the large set of assumptions on which our results are founded, both distributions are not instructive for physics analyses. However, they can be used to define a benchmark point for further phenomenological analyses, in particular for the sensitivity study later on in this article. For later applications, we define the normalisation parameters of our benchmark point to be compatible with these distributions:

$$\zeta(q^2_{\text{max}}) = 0.25\,, \quad \delta_{\text{SL}} = -0.14\,\text{GeV}\,, \tag{3.12}$$

corresponding to a subleading contribution of 14% of the leading-power IW function. This is fully in line with naive power-counting expectations for the subleading-power IW function.

Since the ZRSR cannot provide us with any information on the slopes of either IW function, we have to draw inspiration from elsewhere. Given the lower bound on the slope of the leading-power IW function for $B \to D^{(*)}$ transitions, we assume $\rho, \rho_{\text{SL}} \gtrsim 0.25$. On the other hand, in order to avoid unphysical zero crossings of the IW functions in the semileptonic region in the nominal parametrisation, we need to impose $\rho, \rho_{\text{SL}} \lesssim 0.75$. We choose to use the boundaries to define the slope parameters of our benchmark points as:

$$\rho = 0.25 \qquad \rho_{\text{SL}} = 0.25\,\text{GeV}\,, \tag{3.13}$$

$$\rho = 0.25 \qquad \rho_{\text{SL}} = 0.75\,\text{GeV}\,, \tag{3.14}$$

$$\rho = 0.75 \qquad \rho_{\text{SL}} = 0.75\,\text{GeV}\,, \tag{3.15}$$

$$\rho = 0.75 \qquad \rho_{\text{SL}} = 0.25\,\text{GeV}\,. \tag{3.16}$$

We emphasise again that these values are not viable for any physics analysis, and are merely used when studying the sensitivity to the IW function parameters for upcoming LHCb analyses.

3.3 Observables

The fully differential decay rate of an unpolarised Λ_b to a Λ_c^* with total angular momentum J can be written as

$$\frac{1}{\Gamma_0^{(\ell)}}\frac{\mathrm{d}^2\Gamma_J^{(\ell)}}{\mathrm{d}q^2\,\mathrm{d}\cos\theta_\ell} = \left(a_\ell^{(J)} + b_\ell^{(J)}\cos\theta_\ell + c_\ell^{(J)}\cos^2\theta_\ell\right), \quad \frac{1}{\Gamma_0^{(\ell)}}\frac{\mathrm{d}\Gamma_J^{(\ell)}}{\mathrm{d}q^2} = 2\left(a_\ell^{(J)} + \frac{1}{3}c_\ell^{(J)}\right), \tag{3.17}$$

with coefficient functions $a_\ell^{(J)}(q^2)$, $b_\ell^{(J)}(q^2)$, $c_\ell^{(J)}(q^2)$ for the specific final-state lepton flavour $\ell \in \{e, \mu, \tau\}$. The momentum transfer q^2 is defined as the invariant mass of the leptons in the final state, and θ_ℓ is the helicity angle of the charged lepton with the ℓ-ν_ℓ momentum in the Λ_b rest frame. Our choice of normalisation reads

$$\Gamma_0^{(\ell)}(q^2) = \frac{G_F^2 V_{cb}^2 \sqrt{s_+ s_-}\, m_{\Lambda_c^*}}{96\pi^3 m_{\Lambda_b}^2}\left(1 - \frac{m_\ell^2}{q^2}\right)^2, \tag{3.18}$$

which should not be confused with the total decay width

$$\Gamma_J^{(\ell)} = 2\int_{m_\ell^2}^{(m_{\Lambda_b} - m_{\Lambda_c^*})^2} \mathrm{d}q^2\, \Gamma_0^{(\ell)}(q^2)\left(a_\ell^{(J)}(q^2) + \frac{1}{3}c_\ell^{(J)}(q^2)\right). \tag{3.19}$$

JHEP06(2018)155

From the double-differential rate, we can construct two angular observables in addition to the q^2-differential decay rate: first, the forward-backward asymmetry

$$\begin{aligned} A_{\rm FB}(q^2) &\equiv \frac{1}{\mathrm{d}\Gamma_J^{(\ell)}/\mathrm{d}q^2}\int_{-1}^{+1}\mathrm{d}\cos\theta_\ell\left[\omega_{A_{\rm FB}}(\cos\theta_\ell)\,\frac{\mathrm{d}^2\Gamma_J^{(\ell)}}{\mathrm{d}q^2\,\mathrm{d}\cos\theta_\ell}\right] \\ &= \frac{1}{\mathrm{d}\Gamma_J^{(\ell)}/\mathrm{d}q^2}\,\Gamma_0^{(\ell)}(q^2)b_\ell^{(J)}(q^2)\,, \end{aligned} \tag{3.20}$$

which arises from the term linear in $\cos\theta_\ell$. And secondly, the flat term

$$\begin{aligned} F_{\rm H}(q^2) &\equiv \frac{1}{\mathrm{d}\Gamma_J^{(\ell)}/\mathrm{d}q^2}\int_{-1}^{+1}\mathrm{d}\cos\theta_\ell\left[\omega_{F_{\rm H}}(\cos\theta_\ell)\,\frac{\mathrm{d}^2\Gamma_J^{(\ell)}}{\mathrm{d}q^2\,\mathrm{d}\cos\theta_\ell}\right] \\ &= \frac{1}{\mathrm{d}\Gamma_J^{(\ell)}/\mathrm{d}q^2}\,2\Gamma_0^{(\ell)}(q^2)\left[a_\ell^{(J)}(q^2)+c_\ell^{(J)}(q^2)\right]\,, \end{aligned} \tag{3.21}$$

which arises from a linear combination of the coefficients $a_\ell^{(J)}$ and $c_\ell^{(J)}$ that differs from the one comprising the decay rate eq. (3.19). The weight functions for both observables read:

$$\omega_{A_{\rm FB}}(\cos\theta_\ell)=\frac{3}{2}P_1(\cos\theta_\ell)\,,\quad \omega_{F_{\rm H}}(\cos\theta_\ell)=5P_2(\cos\theta_\ell)+P_0(\cos\theta_\ell)\,. \tag{3.22}$$

In the above, P_n denotes the nth Legendre polynomial.

Note that the definition of the flat term F_H in eq. (3.21) is similar to the one proposed for e.g. the decay $B\to K\ell^+\ell^-$; see ref. [30]. However, contrary to what happens in the mesonic decays in the limit $m_\ell\to 0$, the baryonic F_H does not vanish in the SM. This is due to the fact that the $\Lambda_b\to\Lambda_c^*$ transitions are also mediated by perpendicular polarisation states of the virtual W, which is impossible in the mesonic transitions.

For the decay to the $J=1/2$ final state the coefficients are

$$\begin{aligned} 2a_\ell^{(1/2)} = \Bigg[&|f_{1/2,t}|^2\frac{m_\ell^2}{q^2}(m_{\Lambda_b}-m_{\Lambda_c^*})^2+|f_{1/2,0}|^2(m_{\Lambda_b}+m_{\Lambda_c^*})^2+|f_{1/2,\perp}|^2(m_\ell^2+q^2) \\ &+|g_{1/2,t}|^2\frac{m_\ell^2}{q^2}(m_{\Lambda_b}+m_{\Lambda_c^*})^2+|g_{1/2,0}|^2(m_{\Lambda_b}-m_{\Lambda_c^*})^2+|g_{1/2,\perp}|^2(m_\ell^2+q^2)\Bigg]\,, \end{aligned} \tag{3.23}$$

$$2b_\ell^{(1/2)} = 2\left[f_{1/2,t}f_{1/2,0}+g_{1/2,t}g_{1/2,0}\right]\frac{m_\ell^2}{q^2}(m_{\Lambda_b}^2-m_{\Lambda_c^*}^2)-4\,q^2 f_{1/2,\perp}g_{1/2,\perp}\,, \tag{3.24}$$

$$\begin{aligned} 2c_\ell^{(1/2)} = -\left(1-\frac{m_\ell^2}{q^2}\right)\Bigg[&|f_{1/2,0}|^2(m_{\Lambda_b}+m_{\Lambda_c^*})^2-q^2|f_{1/2,\perp}|^2 \\ &+|g_{1/2,0}|^2(m_{\Lambda_b}-m_{\Lambda_c^*})^2-q^2|g_{1/2,\perp}|^2\Bigg]\,. \end{aligned} \tag{3.25}$$

JHEP06(2018)155

For the $J = 3/2$ we have

$$a_\ell^{(3/2)} = \Big[|F_{1/2,t}|^2 \frac{m_\ell^2}{q^2}(m_{\Lambda_b} - m_{\Lambda_c^*})^2 + |F_{1/2,0}|^2 (m_{\Lambda_b} + m_{\Lambda_c^*})^2 + (|F_{1/2,\perp}|^2 + 3|F_{3/2,\perp}|^2)(m_\ell^2 + q^2) + |G_{1/2,t}|^2 \frac{m_\ell^2}{q^2}(m_{\Lambda_b} + m_{\Lambda_c^*})^2 + |G_{1/2,0}|^2 (m_{\Lambda_b} - m_{\Lambda_c^*})^2 + (|G_{1/2,\perp}|^2 + 3|G_{3/2,\perp}|^2)(m_\ell^2 + q^2) \Big], \tag{3.26}$$

$$b_\ell^{(3/2)} = 2 \left[F_{1/2,t} F_{1/2,0} + G_{1/2,t} G_{1/2,0} \right] \frac{m_\ell^2}{q^2}(m_{\Lambda_b}^2 - m_{\Lambda_c^*}^2) - 4\, q^2 \left[F_{1/2,\perp} G_{1/2,\perp} + 3 F_{3/2,\perp} G_{3/2,\perp} \right], \tag{3.27}$$

$$c_\ell^{(3/2)} = -\left(1 - \frac{m_\ell^2}{q^2}\right) \Big[|F_{1/2,0}|^2 (m_{\Lambda_b} + m_{\Lambda_c^*})^2 - q^2 (|F_{1/2,\perp}|^2 + 3|F_{3/2,\perp}|^2) + |G_{1/2,0}|^2 (m_{\Lambda_b} - m_{\Lambda_c^*})^2 - q^2 (|G_{1/2,\perp}|^2 + 3|G_{3/2,\perp}|^2) \Big]. \tag{3.28}$$

Our results for the angular coefficients in eqs. (3.23)–(3.25) and eqs. (3.26)–(3.28) include the full m_ℓ dependence. We can compare them to the results for the fully differential decay rate in the limit $m_\ell \to 0$ as presented in [18]. We find complete agreement between our limit and the results of [18] when converting to the different basis of form factors as shown in eq. (B.6).

4 Prospects for the determination of the $\Lambda_b^0 \to \Lambda_c^{*+}$ form factors using LHCb data

Similarly to the mesonic $B \to D^{(*)}$ transitions, the most precise SM prediction for $R_{\Lambda_c^*}$ will arise from a combination of theoretical and experimental input. In this section, we investigate the sensitivity to the IW parameters from the decay $\Lambda_b^0 \to \Lambda_c^{*+} \mu^- \bar{\nu}$ in the present and future LHCb datasets when assuming a SM-like distribution.[3] To achieve this, we first produce a series of toy ensembles and subsequently fit the decay distribution to the simulated pseudo events. Estimates for the theoretical uncertainty on $R_{\Lambda_c^*}$ within the SM are then produced based on our fits.

4.1 Experimental situation

Two aspects of the experimental situation are needed to assess the experimental sensitivity. The reconstructed and selected signal yields of the decays $\Lambda_b^0 \to \Lambda_c(2625)^+ \mu^- \bar{\nu}$ and $\Lambda_b^0 \to \Lambda_c(2595)^+ \mu^- \bar{\nu}$ and the resolution in q^2 and $\cos\theta_l$. We estimate the expected signal yields for a given luminosity by extrapolating from the numerical values quoted in ref. [16], taking into the account the increased $b\bar{b}$ cross-section at 13 TeV [31]. We explore the sensitivity to parameters of interest as a function of the luminosity, starting from the current LHCb dataset, up to the luminosity expected at the end of the first LHCb upgrade [32].

A key factor which limits the precision of the experimental measurements is the resolution in q^2 and $\cos\theta_l$, induced by the unreconstructed neutrino. The resolution determines how finely the data is binned and introduces a statistical correlation between adjacent bins.

[3] Note that a popular NP explanation for the present $R_{D^{(*)}}$ anomalies is a rescaling of the coupling associated with effective operator $\sim [\bar{c}\gamma^\mu(1-\gamma_5)b]\,[\bar{\nu}\gamma_\mu(1-\gamma_5)\ell]$. Such a rescaling would leave the angular distribution of $b \to c\ell\bar{\nu}$ decays used here invariant.

JHEP06(2018)155

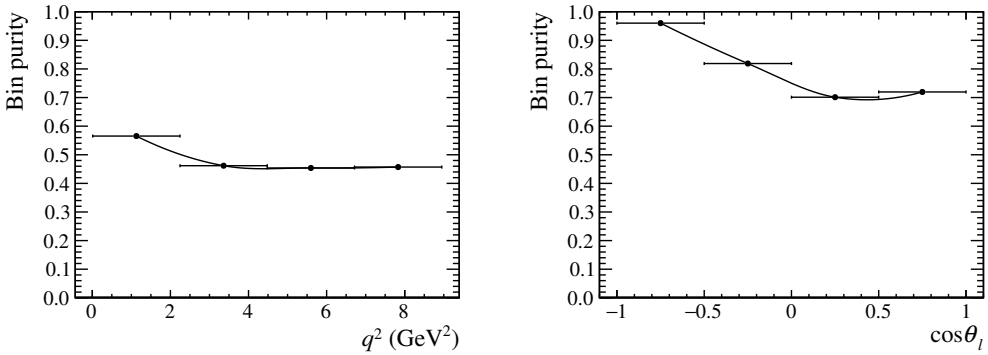

Figure 1. Purity as a function of q^2 and $\cos\theta_l$, defined as the fraction of candidates which belong in a particular kinematic bin. The purity for $\cos\theta_l$ is better than for q^2 due to the better resolution.

At a hadron collider, the momentum of the neutrino can be deduced using the information of the Λ_b^0 flight direction and its mass, up to a two-fold ambiguity. The dominant effects on the resulting resolution originate from the measurement of the primary pp collision and Λ_b^0 vertices, as well the effect of choosing the wrong kinematic solution from the two available. In order to approximate the resolution of the LHCb detector, a sample of $\Lambda_b^0 \to \Lambda_c^{*+}\mu^-\bar{\nu}$ candidates are simulated using Pythia at 13 TeV [33, 34], with a required pseudo-rapidity of $2 < \eta < 5$, approximately corresponding to the LHCb acceptance. The vertices of the pp collision and Λ_b^0 decay are varied according to a resolution inspired from ref. [35] and used in ref. [36]. The resolutions of ± 20 µm in the x and y directions and ± 200 µm in the z direction (defined as the direction aligned with the LHC beam line) is used for the Λ_b^0 vertex. For the pp collision vertex, a resolution of ± 13 µm in x and y and ± 70 µm in z is assumed. With these new vertex positions the two kinematic solutions for the neutrino are then calculated, and one is chosen randomly.

The resulting purities with 4 q^2 bins and 4 $\cos\theta_l$ bins are shown in figure 1, where the purity is defined as the fraction of the number of candidates reconstructed correctly for a given q^2 bin. There is a better purity at negative $\cos\theta_l$, which is due to the interplay between q^2 and $\cos\theta_l$: at high q^2 the $\cos\theta_l$ resolution is poor, and in this region there is a positive $\cos\theta_l$ distribution. The resolution limits the number of bins and induces a statistical correlation between neighbouring bins, which is calculated based on the number of candidates which migrate between those two bins. In the 4×4 bins configuration, this correlation is around 10–30% in both q^2 and $\cos\theta_l$.

In addition to the above, precision measurements of b-hadrons branching fractions at the LHC require a well-measured normalisation channel to cancel the uncertainties related to the production. In principle one could normalise to a well measured B meson decay and take the ratio of production fractions. However, this method would inherit substantial systematic uncertainties, and therefore for this study the decay rate is normalised and only the shape information is used to determine the parameters of interest. This means that the absolute normalisation of the form factors cannot be constrained experimentally. As a consequence we do not report any sensitivity for the form factor parameter $\zeta(q^2_{\rm max})$, which corresponds to this absolute normalisation.

JHEP06(2018)155

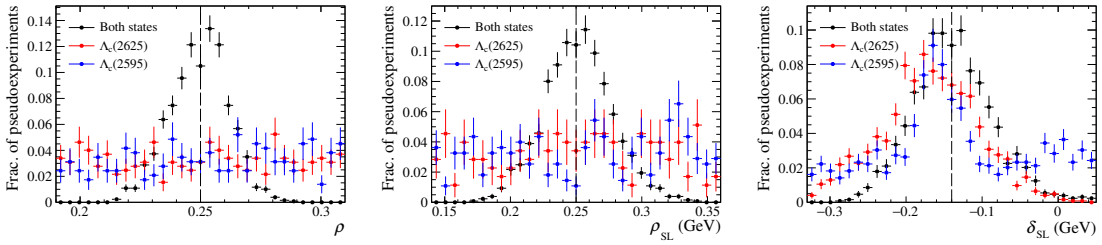

Figure 2. Distribution of the IW parameters as fitted from an ensemble of pseudo-experiments. The distributions are shown for the cases when one of the two Λ_c^{*+} states is fitted, as well as the combination of both. The dashed lines indicate the numerical values of the parameters used to generate the pseudoexperiments.

4.2 Fits to the differential decay rate

For the purpose of this analysis we fix the two HQE parameters $\bar{\Lambda} = m_{\Lambda_b} - m_b$ and $\bar{\Lambda}' = m_{\Lambda_c^*} - m_c$ in the fits.[4] We start by fitting the one-dimensional q^2 distribution of the $\Lambda_b^0 \to \Lambda_c(2625)^+\mu^-\bar{\nu}$ decay, $\Lambda_b^0 \to \Lambda_c(2595)^+\mu^-\bar{\nu}$ decay or a combination thereof. We generate about 300 pseudoexperiments for each parametrisation and benchmark points, and for each pseudoexperiment we generate 50000 $\Lambda_b^0 \to \Lambda_c(2625)^+\mu^-\bar{\nu}$ and 20000 $\Lambda_b^0 \to \Lambda_c(2595)^+\mu^-\bar{\nu}$ events, corresponding to the expected size of the LHCb dataset at the end of the LHC Run II. The resulting one-dimensional distributions of the form factor parameters are shown in figure 2 for the benchmark point described in eq. (3.13). All benchmark points yield similar results. When fitting a single decay mode, we find that there is a degeneracy between the two slope parameters ρ and ρ_{SL} due to a strong correlation that is positive for the $\Lambda_b^0 \to \Lambda_c(2625)^+\mu^-\bar{\nu}$ decay and negative for the $\Lambda_b^0 \to \Lambda_c(2595)^+\mu^-\bar{\nu}$ decay. Only by combining both states in a single fit can the interference between the positive and negative correlation break this degeneracy.

In order to maximise the sensitivity to all three form factor parameters and make full use of the LHCb dataset, we investigate fits to the two-dimensional q^2 and $\cos\theta_l$. The resulting one-dimensional and two-dimensional distributions of the parameters are shown in appendix G. A comparison between the distributions of the IW parameters for the one- and two-dimensional fits is shown in figure 3. The results show that a two-dimensional fit improves the precision on all three parameters with reduced correlations between them, as shown in figure 6. This strongly motivates a full two-dimensional fit to both Λ_c^{*+} states simultaneously for any future LHCb analysis to give the best possible precision on the form factor parameters.

4.3 Projected precision on the $R_{\Lambda_c^*}$ predictions

Finally, by using the expected precision on the form factors, one can calculate the precision on the ratio $R_{\Lambda_c^*}$, which denotes both the $R_{\Lambda_c(2595)^+}$ and $R_{\Lambda_c(2625)^+}$ ratios as they are

[4]For upcoming experimental analyses, however, we recommend to let these parameters float in order to reflect theoretical ambiguities in their definitions. The concrete window should reflect the definition of the heavy-quark mass used in the fit.

JHEP06(2018)155

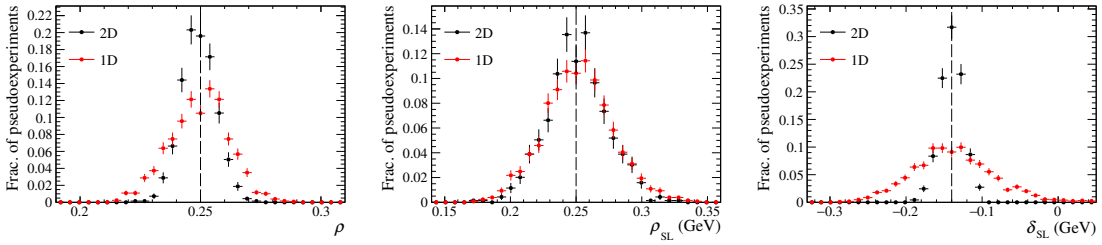

Figure 3. Distribution of the IW parameters as fitted from an ensemble of pseudo-experiments. The sensitivity is shown for fits to both the one-dimensional q^2 and two-dimensional $q^2 \times \cos\theta_l$ distributions. The dashed lines indicate the numerical values of the parameters used to generate the pseudoexperiments.

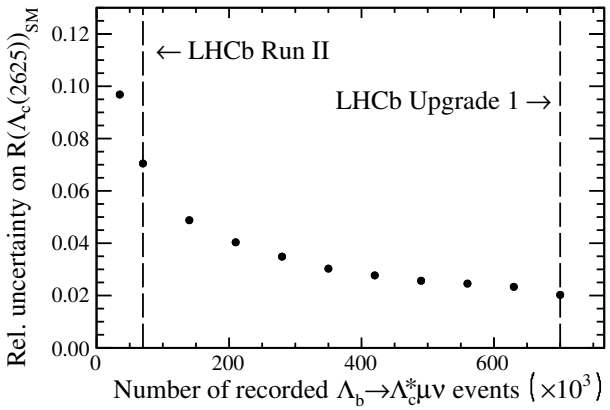

Figure 4. Expected theoretical precision of the $R_{\Lambda_c(2625)^+}$ ratio as a function of the amount of $\Lambda_b^0 \to \Lambda_c^{*+}\mu\nu$ events recorded by the LHCb experiment. The yields expected at the end of the LHC Run II and after the LHCb upgrade 1 are highlighted by the vertical lines.

derived from the same parameters and therefore have similar uncertainties. We carry out our study for each of the two paramatrisations of the IW functions given in section 3.1, and each of the common benchmark points defined in section 3.2. The precision as a function of the luminosity collected by the LHCb experiment is shown in figure 4, where in order to be conservative and ensure the legibility of our results we only show the worst case of our studies. Assuming the exponential model[5] describes the data well, a statistical precision of $\sim 7\%$ can be expected from run I+II data. A reduction to $\sim 2\%$ can be expected after upgrade 1 of the LHCb detector. For the linear model, we find in general smaller uncertainties than for the exponential model. Our estimates for the uncertainties ignore power suppressed terms in the HQET expansion and experimental systematic uncertainties, which could become relevant at that level of precision.

Similar to what has been done in the literature for R_{D^*}, we can estimate the impact of the dominant unknown $1/m_c^2$ corrections to the HQET relations on the theory predictions

[5]With exponential model we indicate the exponential parametrisation described in section 3.1 together with the benchmark points obtained in section 3.2.

JHEP06(2018)155

for the $R_{\Lambda_c^*}$. Following the discussion [37], we wish to separate the term involving the timelike form factors from the term that can be taken directly from data on the semimuonic decay mode. We therefore decompose

$$\frac{\mathrm{d}\Gamma_J^{(\tau)}}{\mathrm{d}q^2} = \frac{\mathrm{d}\Gamma_J^{(\tau,1)}}{\mathrm{d}q^2} + \frac{\mathrm{d}\Gamma_J^{(\tau,2)}}{\mathrm{d}q^2} \tag{4.1}$$

in two contributions

$$\frac{\mathrm{d}\Gamma_J^{(\tau,1)}}{\mathrm{d}q^2} = \frac{1}{3}\left(1-\frac{m_\tau^2}{q^2}\right)^2\left(2+\frac{m_\tau^2}{q^2}\right)\frac{\mathrm{d}\Gamma^{(\ell)}}{q^2}\bigg|_{m_\ell\to 0}, \tag{4.2}$$

$$\frac{\mathrm{d}\Gamma_J^{(\tau,2)}}{\mathrm{d}q^2} = \begin{cases} \Gamma_0^{(\tau)}\left[|f_{1/2,t}|^2\frac{m_\tau^2}{q^2}\left(m_{\Lambda_b}-m_{\Lambda_c^*}\right)^2+|g_{1/2,t}|^2\frac{m_\tau^2}{q^2}\left(m_{\Lambda_b}+m_{\Lambda_c^*}\right)^2\right] & J=1/2 \\ 2\Gamma_0^{(\tau)}\left[|F_{1/2,t}|^2\frac{m_\tau^2}{q^2}\left(m_{\Lambda_b}-m_{\Lambda_c^*}\right)^2+|G_{1/2,t}|^2\frac{m_\tau^2}{q^2}\left(m_{\Lambda_b}+m_{\Lambda_c^*}\right)^2\right] & J=3/2 \end{cases}. \tag{4.3}$$

Note here that the $(\tau,1)$ terms are taken directly from data, while the $(\tau,2)$ terms rely on the HQET relations between the form factors for theoretical predictions. Correspondingly, we then decompose $R_{\Lambda_c^*} = R_{\Lambda_c^*,1} + R_{\Lambda_c^*,2}$ with

$$R_{\Lambda_c^*(J),i} = \frac{\int_{m_\tau^2}^{(m_{\Lambda_b}-m_{\Lambda_c^*})^2}\mathrm{d}q^2\,\frac{\mathrm{d}\Gamma_J^{(\tau,i)}}{\mathrm{d}q^2}}{\int_{m_\mu^2}^{(m_{\Lambda_b}-m_{\Lambda_c^*})^2}\mathrm{d}q^2\,\frac{\mathrm{d}\Gamma_J^{(\mu)}}{\mathrm{d}q^2}}. \tag{4.4}$$

We find that the relative contribution by the $(\tau,1)$ term is both dominant and stable under variation of the slope parameters across our four benchmark points in the exponential model. We find that

$$R_{\Lambda_c(2595),1} \simeq 0.76\cdot R_{\Lambda_c(2595)^+}, \qquad \text{and} \qquad R_{\Lambda_c(2625),1} \simeq 0.77\cdot R_{\Lambda_c(2625)^+}. \tag{4.5}$$

For a conservative estimate, we can assume that the $1/m_c^2$ contributions yield 30% corrections to the HQET relations as estimated in [37]. Consequently, we would face an inherent theory uncertainty of $\sim 8\%$ for $R_{\Lambda_c(2595)}$ and up to $\sim 7\%$ for $R_{\Lambda_c(2625)}$.[6] Given that projected statistical uncertainty in figure 4 are of similar size already with the full run II dataset, we come to the conclusion that our theoretical uncertainty estimates strongly motivate dedicated lattice QCD studies of the $\Lambda_b \to \Lambda_c^*$ form factors.

5 Conclusion

Motivated by the recent deviations in LFU in semileptonic $b\to s$ and $b\to c$ decays, we have provided the theoretical ingredients needed to constrain the theoretical uncertainty of the lepton universality ratios $R_{\Lambda_c(2595)^+}$ and $R_{\Lambda_c(2625)^+}$, collectively denoted as $R_{\Lambda_c^*}$.

To this end, we have improved and extended upon the work in [18]. We provide a new definition of the hadronic form factors, convenient for the decay observables, and work out

[6] Switching the b and c quark mass schemes from the pole to the kinetic scheme yields a shift in $R_{\Lambda_c^*}$ by less then 4%. The scheme dependence, and therefore the values of the heavy-quark expansion parameters $\bar{\Lambda}$ and $\bar{\Lambda}'$ are presently inconsequential compared to the inherent $1/m_c^2$ uncertainty.

JHEP06(2018)155

formulae for $\mathcal{O}(\alpha_s)$ corrections to HQE. We then propose a parameterisation of the Isgur-Wise function informed from previous studies on the ground state $\Lambda_b^0 \to \Lambda_c^+$ transition [22] and perform a zero recoil sum rule to provide a benchmark point for these parameters to be used in a study of the sensitivity to these parameters for a future analysis of LHCb data. Last but not least, we provide the finite lepton mass terms for the two double differential decay distributions.

We investigated the benefits of fitting the two-dimensional $q^2 - \cos\theta_l$ distribution over fitting only the q^2 distribution, for either of the Λ_c^{*+} hadronic states and their combination. We find that fitting the angular information in addition to the q^2 spectrum is crucial to obtain sensitivity to the sub-leading Igsur-Wise function. In addition, we stress that a combined analysis of both Λ_c^{*+} states is necessary to break the degeneracy between the slopes of the leading and sub-leading Igsur-Wise functions. Finally, we show that by measuring the differential decay rate of $\Lambda_b^0 \to \Lambda_c^{*+}\mu^-\bar{\nu}$, small statistical uncertainty for a data driven determination of the $R_{\Lambda_c^*}$ ratios can be achieved. Our results therefore motivate an LHCb analysis of the $\Lambda_b^0 \to \Lambda_c^{*+}\mu^-\bar{\nu}$ double-differential decay rate and the subsequent experimental measurement of the $R_{\Lambda_c^*}$ ratios. On the other hand, we also demonstrate that the unknown $1/m^2$ terms in the form factors' expansion produce at present an irreducible uncertainty that is of the same order as the statistical uncertainty. This motivates further theoretical studies of the form factors, e.g. from lattice QCD.

Acknowledgments

We thank Marcin Chrzaszcz, Gino Isidori, Zoltan Ligeti, and Nicola Serra for helpful and enjoyable discussions. P.B. acknowledges support by the Bundesministerium für Bildung und Forschung (BMBF), and by the Deutsche Forschungsgemeinschaft (DFG) within Research Unit FOR 1873 (Quark Flavour Physics and Effective Field Theories). D.v.D. gratefully acknowledges partial support by the Swiss National Science Foundation (SNF) under contract 200021-159720, and by the Deutsche Forschungsgemeinschaft (DFG) within the Emmy Noether programme under grant DY 130/1-1 and through the DFG Collaborative Research Center 110 "Symmetries and the Emergence of Structure in QCD. The work of M.B. and P.O. is supported in part by the Swiss National Science Foundation (SNF) under contracts 200021-159720 and BSSGI0_155990, respectively. The authors gratefully acknowledge the compute and data resources provided by the Leibniz Supercomputing Centre.

A Details on the Rarita-Schwinger object

We describe a $J^P = 3/2^-$ state by the spin-3/2 projection u^α of a generic Rarita-Schwinger object $u^\alpha_{\rm RS}(k,\eta) = \eta^\alpha u(k)$,

$$\begin{aligned} u^\alpha_{(3/2)}(k,\eta,s_c) &= \left[\eta^\alpha - \frac{1}{3}\left(\gamma^\alpha + \frac{k^\alpha}{m_{\Lambda_c^*}}\right)\not{\eta}\right] u(k,s_c) \\ &= \left[g^\alpha{}_\beta - \frac{1}{3}\left(\gamma^\alpha + \frac{k^\alpha}{m_{\Lambda_c^*}}\right)\gamma_\beta\right] u^\beta_{\rm RS}(k,\eta(\lambda),s_c) \\ &\equiv \left[P_{3/2}\right]^\alpha{}_\beta\, u^\beta_{\rm RS}(k,\eta(\lambda),s_c)\,. \end{aligned} \tag{A.1}$$

In the above, $u(k, s_c)$ denotes a spin-$1/2^+$ spinor of four momentum k and rest-frame helicity $s_c = \pm 1/2$, and η denotes a polarisation vector with $J^P = 1^-$. Likewise, we can also characterise the $J^P = 1/2^-$ state in term of the projection onto the spin-1/2 component as:

$$u^{\alpha}_{(1/2)}(k, \eta, s_c) = \frac{1}{3}\left[\gamma^{\alpha} + \frac{k^{\alpha}}{m_{\Lambda_c^*}}\right] \not{\eta}\; u(k, s_c) \tag{A.2}$$

$$= \frac{1}{3}\left[\gamma^{\alpha} + \frac{k^{\alpha}}{m_{\Lambda_c^*}}\right] \gamma_{\beta}\; u^{\beta}_{\mathrm{RS}}(k, \eta(\lambda), s_c) \tag{A.3}$$

$$\equiv \left[P_{1/2}\right]^{\alpha}{}_{\beta}\, u^{\beta}_{\mathrm{RS}}(k, \eta(\lambda), s_c)\,. \tag{A.4}$$

The Rarita-Schwinger object fulfills the equation of motion

$$\left[i\varepsilon_{\mu\alpha\beta\sigma}\gamma^5\gamma^{\mu}k^{\sigma} + im\,\sigma_{\alpha\beta}\right] u^{\beta}(k) = 0\,. \tag{A.5}$$

By virtue of the equations of motions, the following identities hold

$$k^{\alpha}u^{\mathrm{RS}}_{\alpha}(k, \eta, s_c) = 0 = \eta(t)^{\alpha}u^{\mathrm{RS}}_{\alpha}(k, \eta, s_c) \tag{A.6}$$

while for the spin 3/2 projection u_{α} of a Rarita-Schwinger object, the following relations are also true:

$$\gamma^{\alpha}u^{(3/2)}_{\alpha}(k, \eta, s_c) = 0\,, \tag{A.7}$$

$$-i\sigma^{\alpha\beta}\, u^{(3/2)}_{\alpha}(k, \eta, s_c) = u^{\beta}_{(3/2)}(k, \eta, s_c)\,. \tag{A.8}$$

The completeness relation for the 3/2 spinor read

$$\sum_{\lambda(\prime), s_c(\prime)} u^{\alpha}_{3/2}(k, \eta(\lambda), s_c)\bar{u}^{\alpha'}_{3/2}(k, \eta(\lambda'), s'_c)$$

$$= (\not{k} + m_{\Lambda_c^*})\left[-g^{\alpha\alpha'} + \frac{k^{\alpha}k^{\alpha'}}{m^2_{\Lambda_c^*}} + \frac{1}{3}\left(\gamma^{\alpha} - \frac{k^{\alpha}}{m_{\Lambda_c^*}}\right)\left(\gamma^{\alpha'} + \frac{k^{\alpha'}}{m_{\Lambda_c^*}}\right)\right], \tag{A.9}$$

while for the 1/2 spinor we have:

$$\sum_{\lambda(\prime), s_c(\prime)} u^{\alpha}_{1/2}(k, \eta(\lambda), s_c)\bar{u}^{\alpha'}_{1/2}(k, \eta(\lambda'), s'_c) = -\frac{1}{3}(\not{k} + m_{\Lambda_c^*})\left(\gamma^{\alpha} - \frac{k^{\alpha}}{m_{\Lambda_c^*}}\right)\left(\gamma^{\alpha'} + \frac{k^{\alpha'}}{m_{\Lambda_c^*}}\right) \tag{A.10}$$

B Details on the form factor definitions

The spin structures $\Gamma^{\alpha\mu}_{J,i}$ that contribute to the transition $\Lambda_b \to \Lambda_c^*$ are listed in the following.

For the final state $\Lambda_c(2595)^+$ and for the vector current ($J = V$) we find:

$$\Gamma^{\alpha\mu}_{V,(1/2,t)} = \frac{\sqrt{4m_{\Lambda_b}m_{\Lambda_c^*}}}{\sqrt{s_+}}\frac{2m_{\Lambda_c^*}}{\sqrt{s_+s_-}}p^{\alpha}\,\frac{m_{\Lambda_b} - m_{\Lambda_c^*}}{\sqrt{q^2}}\,\frac{q^{\mu}}{\sqrt{q^2}}\,,$$

$$\Gamma^{\alpha\mu}_{V,(1/2,0)} = \frac{\sqrt{4m_{\Lambda_b}m_{\Lambda_c^*}}}{\sqrt{s_-}}\frac{2m_{\Lambda_c^*}}{\sqrt{s_+s_-}}p^{\alpha}\,\frac{m_{\Lambda_b} + m_{\Lambda_c^*}}{s_+}\left[(p+k)^{\mu} - \frac{m^2_{\Lambda_b} - m^2_{\Lambda_c^*}}{q^2}q^{\mu}\right], \tag{B.1}$$

$$\Gamma^{\alpha\mu}_{V,(1/2,\perp)} = \frac{\sqrt{4m_{\Lambda_b}m_{\Lambda_c^*}}}{\sqrt{s_-}}\frac{2m_{\Lambda_c^*}}{\sqrt{s_+s_-}}p^{\alpha}\,\left[\gamma^{\mu} - \frac{2m_{\Lambda_c^*}}{s_+}p^{\mu} - \frac{2m_{\Lambda_b}}{s_+}k^{\mu}\right],$$

JHEP06(2018)155

while for the axialvector current ($J = A$) we obtain:

$$\begin{aligned}
\Gamma^{\alpha\mu}_{A,(1/2,t)} &= \frac{\sqrt{4m_{\Lambda_b}m_{\Lambda_c^*}}}{\sqrt{s_-}}\frac{2m_{\Lambda_c^*}}{\sqrt{s_+s_-}}p^\alpha\,\frac{m_{\Lambda_b}+m_{\Lambda_c^*}}{\sqrt{q^2}}\,\frac{q^\mu}{\sqrt{q^2}}\,,\\
\Gamma^{\alpha\mu}_{A,(1/2,0)} &= \frac{\sqrt{4m_{\Lambda_b}m_{\Lambda_c^*}}}{\sqrt{s_+}}\frac{2m_{\Lambda_c^*}}{\sqrt{s_+s_-}}p^\alpha\,\frac{m_{\Lambda_b}-m_{\Lambda_c^*}}{s_-}\left[(p+k)^\mu-\frac{m^2_{\Lambda_b}-m^2_{\Lambda_c^*}}{q^2}q^\mu\right]\,,\\
\Gamma^{\alpha\mu}_{A,(1/2,\perp)} &= \frac{\sqrt{4m_{\Lambda_b}m_{\Lambda_c^*}}}{\sqrt{s_+}}\frac{2m_{\Lambda_c^*}}{\sqrt{s_+s_-}}p^\alpha\left[\gamma^\mu+\frac{2m_{\Lambda_c^*}}{s_-}p^\mu-\frac{2m_{\Lambda_b}}{s_-}k^\mu\right]\,.
\end{aligned}\tag{B.2}$$

In the case of the final state $\Lambda_c(2625)^+$, for the vector current ($J = V$) we obtain:

$$\begin{aligned}
\Gamma^{\alpha\mu}_{V,(1/2,t)} &= \frac{\sqrt{4m_{\Lambda_b}m_{\Lambda_c^*}}}{\sqrt{s_+}}\frac{2m_{\Lambda_c^*}}{\sqrt{s_+s_-}}p^\alpha\,\frac{m_{\Lambda_b}-m_{\Lambda_c^*}}{\sqrt{q^2}}\,\frac{q^\mu}{\sqrt{q^2}}\,,\\
\Gamma^{\alpha\mu}_{V,(1/2,0)} &= \frac{\sqrt{4m_{\Lambda_b}m_{\Lambda_c^*}}}{\sqrt{s_-}}\frac{2m_{\Lambda_c^*}}{\sqrt{s_+s_-}}p^\alpha\,\frac{m_{\Lambda_b}+m_{\Lambda_c^*}}{s_+}\left[(p+k)^\mu-\frac{m^2_{\Lambda_b}-m^2_{\Lambda_c^*}}{q^2}q^\mu\right]\,,\\
\Gamma^{\alpha\mu}_{V,(1/2,\perp)} &= \frac{\sqrt{4m_{\Lambda_b}m_{\Lambda_c^*}}}{\sqrt{s_-}}\frac{2m_{\Lambda_c^*}}{\sqrt{s_+s_-}}p^\alpha\left[\gamma^\mu-\frac{2m_{\Lambda_c^*}}{s_+}p^\mu-\frac{2m_{\Lambda_b}}{s_+}k^\mu\right]\,,\\
\Gamma^{\alpha\mu}_{V,(3/2,\perp)} &= \frac{\sqrt{4m_{\Lambda_b}m_{\Lambda_c^*}}}{\sqrt{s_-}}\frac{-4i\varepsilon^{\alpha\mu pk}}{\sqrt{s_+s_-}}\gamma_5+\Gamma_{V,(1/2,\perp)}\,,
\end{aligned}\tag{B.3}$$

while for the axialvector current ($J = A$) we use

$$\begin{aligned}
\Gamma^{\alpha\mu}_{A,(1/2,t)} &= \frac{\sqrt{4m_{\Lambda_b}m_{\Lambda_c^*}}}{\sqrt{s_-}}\frac{2m_{\Lambda_c^*}}{\sqrt{s_+s_-}}p^\alpha\,\frac{m_{\Lambda_b}+m_{\Lambda_c^*}}{\sqrt{q^2}}\,\frac{q^\mu}{\sqrt{q^2}}\,,\\
\Gamma^{\alpha\mu}_{A,(1/2,0)} &= \frac{\sqrt{4m_{\Lambda_b}m_{\Lambda_c^*}}}{\sqrt{s_+}}\frac{2m_{\Lambda_c^*}}{\sqrt{s_+s_-}}p^\alpha\,\frac{m_{\Lambda_b}-m_{\Lambda_c^*}}{s_-}\left[(p+k)^\mu-\frac{m^2_{\Lambda_b}-m^2_{\Lambda_c^*}}{q^2}q^\mu\right]\,,\\
\Gamma^{\alpha\mu}_{A,(1/2,\perp)} &= \frac{\sqrt{4m_{\Lambda_b}m_{\Lambda_c^*}}}{\sqrt{s_+}}\frac{2m_{\Lambda_c^*}}{\sqrt{s_+s_-}}p^\alpha\left[\gamma^\mu+\frac{2m_{\Lambda_c^*}}{s_-}p^\mu-\frac{2m_{\Lambda_b}}{s_-}k^\mu\right]\,,\\
\Gamma^{\alpha\mu}_{A,(3/2,\perp)} &= \frac{\sqrt{4m_{\Lambda_b}m_{\Lambda_c^*}}}{\sqrt{s_+}}\frac{-4i\varepsilon^{\alpha\mu pk}}{\sqrt{s_+s_-}}\gamma_5-\Gamma_{A,(1/2,\perp)}\,.
\end{aligned}\tag{B.4}$$

Note that we adopted the convention $\varepsilon^{0123} = -\varepsilon_{0123} = +1$ for the Levi-Civita tensor.

In the above a recurring term fulfills

$$\bar{u}_\alpha(k)\frac{-2m_{\Lambda_c^*}}{\sqrt{s_+s_-}}p^\alpha = \bar{u}_\alpha(k)\eta^\alpha(0)\,.\tag{B.5}$$

To conclude, we also provide the matching between our form factor definitions and the

JHEP06(2018)155

ones in [18]:

$$
\begin{aligned}
F_{1/2,t}(q^2(w)) &= +\frac{\sqrt{w-1}}{\sqrt{2}(r-1)}(w+1)\left[(r-1)l_{V_1}+(rw-1)l_{V_2}+(r-w)l_{V_3}-l_{V_4}\right] ,\\
F_{1/2,0}(q^2(w)) &= +\frac{\sqrt{w+1}}{\sqrt{2}(1+r)}\left[(r+1)(w-1)l_{V_1}+(w^2-1)(rl_{V_2}+l_{V_3})+(w-r)l_{V_4}\right] ,\\
F_{1/2,\perp}(q^2(w)) &= -\frac{\sqrt{w+1}}{2\sqrt{2}}\left[2(1-w)l_{V_1}+l_{V_4}\right] ,\\
F_{3/2,\perp}(q^2(w)) &= -\frac{\sqrt{w+1}}{2\sqrt{2}}l_{V_4} ,\\
G_{1/2,t}(q^2(w)) &= +\frac{\sqrt{w+1}}{\sqrt{2}(r+1)}(w-1)\left[(r+1)l_{A_1}+(rw-1)l_{A_2}+(r-w)l_{A_3}-l_{A_4}\right] ,\\
G_{1/2,0}(q^2(w)) &= +\frac{\sqrt{w-1}}{\sqrt{2}(1-r)}\left[(r-1)(w+1)l_{A_1}+(w^2-1)(rl_{A_2}+l_{A_3})+(w-r)l_{A_4}\right] ,\\
G_{1/2,\perp}(q^2(w)) &= -\frac{\sqrt{w-1}}{2\sqrt{2}}\left[-2(1+w)l_{A_1}+l_{A_4}\right] ,\\
G_{3/2,\perp}(q^2(w)) &= +\frac{\sqrt{w-1}}{2\sqrt{2}}l_{A_4} ,
\end{aligned}
\tag{B.6}
$$

with $r = m_{\Lambda_c^*}/m_{\Lambda_b}$.

We worked out the matching between our convention and [18] also for the form factors of $\Lambda_b \to \Lambda_c(2595)^+$ transitions. This is slightly more involved since our approach and the approach of [18] for the spin $1/2^-$ projection of the Rarita-Schwinger object differ. We find it convenient to use:

$$
\sum_{\lambda_c',s_c'} C^{1/2,s_c}_{\lambda_c',s_c'}\,\bar{u}^{(1/2)}_{\alpha}(k,\eta(\lambda_c'),s_c')p^{\alpha} = -\frac{1}{\sqrt{3}}\bar{u}(k,s_c)\gamma^5\left(\frac{1}{m_{\Lambda_c^*}}k\cdot q+\not{q}\right) , \tag{B.7}
$$

with the $C^{1/2,s_c}_{\lambda_c',s_c'}$ being the Clebsch-Gordan coefficients for $j_1 \oplus j_2 = 1 \oplus 1/2$ angular momentum. Using eq. (B.7), the matching between our form factors for the $\Lambda_b \to \Lambda_c(2595)^+$ transition and the ones in [18] reads:

$$
\begin{aligned}
f_{1/2,t}(q^2(w)) &= +\sqrt{\frac{3}{2}}\frac{\sqrt{w-1}}{r-1}\left[(r+1)d_{V_1}+(rw-1)d_{V_2}+(r-w)d_{V_3}\right] ,\\
f_{1/2,0}(q^2(w)) &= +\sqrt{\frac{3}{2}}\frac{\sqrt{w+1}}{r+1}\left[(r-1)d_{V_1}+(w-1)(rd_{V_2}+d_{V_3})\right] ,\\
f_{1/2,\perp}(q^2(w)) &= -\sqrt{\frac{3}{2}}\sqrt{w+1}\,d_{V_1} ,\\
g_{1/2,t}(q^2(w)) &= +\sqrt{\frac{3}{2}}\frac{\sqrt{w+1}}{r+1}\left[(r-1)d_{A_1}+(rw-1)d_{A_2}+(r-w)d_{A_3}\right] ,\\
g_{1/2,0}(q^2(w)) &= +\sqrt{\frac{3}{2}}\frac{\sqrt{w-1}}{r-1}\left[(r+1)d_{A_1}+(w+1)(rd_{A_2}+d_{A_3})\right] ,\\
g_{1/2,\perp}(q^2(w)) &= -\sqrt{\frac{3}{2}}\sqrt{w-1}\,d_{A_1} .
\end{aligned}
\tag{B.8}
$$

JHEP06(2018)155

C Helicity amplitudes

C.1 $1/2^+ \to 1/2^-$

For the scalar current, defined as

$$h_S^\alpha(s_b, s_c, \lambda_c) \equiv \bar{u}^\alpha(k, \eta(\lambda_c), s_c) u(p, s_b)\,, \tag{C.1}$$

we find the following non vanishing terms:

$$\frac{1}{\sqrt{2}} h_S^\alpha(-1/2, -1/2, +1) = h_S^\alpha(-1/2, +1/2, 0) = \frac{\sqrt{2}}{3}\sqrt{s_+}\eta^{*\alpha}(+1)\,, \tag{C.2}$$

$$\frac{1}{\sqrt{2}} h_S^\alpha(+1/2, +1/2, -1) = h_S^\alpha(+1/2, -1/2, 0) = \frac{\sqrt{2}}{3}\sqrt{s_+}\eta^{*\alpha}(-1)\,, \tag{C.3}$$

$$-h_S^\alpha(+1/2, -1/2, +1) = \sqrt{2} h_S^\alpha(+1/2, +1/2, 0) = \frac{\sqrt{2}}{3}\sqrt{s_+}\eta^{*\alpha}(0)\,, \tag{C.4}$$

$$-h_S^\alpha(-1/2, +1/2, -1) = \sqrt{2} h_S^\alpha(-1/2, -1/2, 0) = \frac{\sqrt{2}}{3}\sqrt{s_+}\eta^{*\alpha}(0)\,. \tag{C.5}$$

For the pseudoscalar current, defined as

$$h_P^\alpha(s_b, s_c, \lambda_c) \equiv \bar{u}^\alpha(k, \eta(\lambda_c), s_c)\gamma_5 u(p, s_b)\,, \tag{C.6}$$

one finds:

$$\frac{1}{\sqrt{2}} h_P^\alpha(-1/2, -1/2, +1) = -h_P^\alpha(-1/2, +1/2, 0) = +\frac{\sqrt{2}}{3}\sqrt{s_-}\eta^{*\alpha}(+1)\,, \tag{C.7}$$

$$-\frac{1}{\sqrt{2}} h_P^\alpha(+1/2, +1/2, -1) = h_P^\alpha(+1/2, -1/2, 0) = +\frac{\sqrt{2}}{3}\sqrt{s_-}\eta^{*\alpha}(-1)\,, \tag{C.8}$$

$$h_P^\alpha(+1/2, -1/2, +1) = -\sqrt{2} h_P^\alpha(+1/2, +1/2, 0) = +\frac{\sqrt{2}}{3}\sqrt{s_-}\eta^{*\alpha}(0)\,, \tag{C.9}$$

$$-h_P^\alpha(-1/2, +1/2, -1) = \sqrt{2} h_P^\alpha(-1/2, -1/2, 0) = +\frac{\sqrt{2}}{3}\sqrt{s_-}\eta^{*\alpha}(0)\,. \tag{C.10}$$

For the vector current

$$h_{V,\lambda_q}^\alpha(s_b, s_c, \lambda_c) \equiv \bar{u}^\alpha(k, \eta(\lambda_c), s_c) \not{\epsilon}^*(\lambda_q) u(p, s_b)\,, \tag{C.11}$$

we identify

$$h_{V,t}^\alpha(s_b, s_c, \lambda_c) = \frac{m_{\Lambda_b} - m_{\Lambda_c^*}}{\sqrt{q^2}} h_S^\alpha(s_b, s_c, \lambda_c)\,. \tag{C.12}$$

For the transverse polarisation we find:

$$-\frac{1}{\sqrt{2}} h_{V,-1}^\alpha(+1/2, -1/2, +1) = h_{V,-1}^\alpha(+1/2, +1/2, 0) = +\frac{2}{3}\sqrt{s_-}\eta^{*\alpha}(+1)\,, \tag{C.13}$$

$$-\frac{1}{\sqrt{2}} h_{V,+1}^\alpha(-1/2, +1/2, -1) = h_{V,+1}^\alpha(-1/2, -1/2, 0) = +\frac{2}{3}\sqrt{s_-}\eta^{*\alpha}(-1)\,, \tag{C.14}$$

$$h_{V,+1}^\alpha(-1/2, -1/2, +1) = -\sqrt{2} h_{V,+1}^\alpha(-1/2, +1/2, 0) = +\frac{2}{3}\sqrt{s_-}\eta^{*\alpha}(0)\,, \tag{C.15}$$

$$h_{V,-1}^\alpha(+1/2, +1/2, -1) = -\sqrt{2} h_{V,-1}^\alpha(+1/2, -1/2, 0) = +\frac{2}{3}\sqrt{s_-}\eta^{*\alpha}(0)\,. \tag{C.16}$$

JHEP06(2018)155

For the longitudinal polarisation we find:

$$\frac{1}{\sqrt{2}}h^{\alpha}_{V,0}(-1/2,-1/2,+1) = -h^{\alpha}_{V,0}(-1/2,+1/2,0) = \frac{\sqrt{2}}{3}\frac{m_{\Lambda_b}+m_{\Lambda_c^*}}{\sqrt{q^2}}\sqrt{s_-}\eta^{*\alpha}(+1)\,, \quad \text{(C.17)}$$

$$\frac{1}{\sqrt{2}}h^{\alpha}_{V,0}(+1/2,+1/2,-1) = -h^{\alpha}_{V,0}(+1/2,-1/2,0) = \frac{\sqrt{2}}{3}\frac{m_{\Lambda_b}+m_{\Lambda_c^*}}{\sqrt{q^2}}\sqrt{s_-}\eta^{*\alpha}(-1)\,, \quad \text{(C.18)}$$

$$-h^{\alpha}_{V,0}(+1/2,-1/2,+1) = \sqrt{2}h^{\alpha}_{V,0}(+1/2,+1/2,0) = \frac{\sqrt{2}}{3}\frac{m_{\Lambda_b}+m_{\Lambda_c^*}}{\sqrt{q^2}}\sqrt{s_-}\eta^{*\alpha}(0)\,, \quad \text{(C.19)}$$

$$-h^{\alpha}_{V,0}(-1/2,+1/2,-1) = \sqrt{2}h^{\alpha}_{V,0}(-1/2,-1/2,0) = \frac{\sqrt{2}}{3}\frac{m_{\Lambda_b}+m_{\Lambda_c^*}}{\sqrt{q^2}}\sqrt{s_-}\eta^{*\alpha}(0)\,. \quad \text{(C.20)}$$

Similarly for the axialvector current

$$h^{\alpha}_{A,\lambda_q}(s_b,s_c,\lambda_c) \equiv \bar{u}^{\alpha}(k,\eta(\lambda_c),s_c)\not{\epsilon}^*(\lambda_q)\gamma_5 u(p,s_b)\,, \quad \text{(C.21)}$$

we identify

$$h^{\alpha}_{A,t}(s_b,s_c,\lambda_c) = -\frac{m_{\Lambda_b}+m_{\Lambda_c^*}}{\sqrt{q^2}}h^{\alpha}_{P}(s_b,s_c,\lambda_c)\,. \quad \text{(C.22)}$$

For the transverse polarisation we find

$$\frac{1}{\sqrt{2}}h^{\alpha}_{A,-1}(+1/2,-1/2,+1) = -h^{\alpha}_{A,-1}(+1/2,+1/2,0) = +\frac{2}{3}\sqrt{s_+}\eta^{*\alpha}(+1)\,, \quad \text{(C.23)}$$

$$-\frac{1}{\sqrt{2}}h^{\alpha}_{A,+1}(-1/2,+1/2,-1) = h^{\alpha}_{A,+1}(-1/2,-1/2,0) = +\frac{2}{3}\sqrt{s_+}\eta^{*\alpha}(-1)\,, \quad \text{(C.24)}$$

$$h^{\alpha}_{A,+1}(-1/2,-1/2,+1) = -\sqrt{2}h^{\alpha}_{A,+1}(-1/2,+1/2,0) = +\frac{2}{3}\sqrt{s_+}\eta^{*\alpha}(0)\,, \quad \text{(C.25)}$$

$$-h^{\alpha}_{A,-1}(+1/2,+1/2,-1) = \sqrt{2}h^{\alpha}_{A,-1}(+1/2,-1/2,0) = +\frac{2}{3}\sqrt{s_+}\eta^{*\alpha}(0)\,. \quad \text{(C.26)}$$

For the longitudinal polarisation we find

$$-\frac{1}{\sqrt{2}}h^{\alpha}_{A,0}(-1/2,-1/2,+1) = h^{\alpha}_{A,0}(-1/2,+1/2,0) = +\frac{\sqrt{2}}{3}\frac{m_{\Lambda_b}-m_{\Lambda_c^*}}{\sqrt{q^2}}\sqrt{s_+}\eta^{*\alpha}(+1)\,, \quad \text{(C.27)}$$

$$\frac{1}{\sqrt{2}}h^{\alpha}_{A,0}(+1/2,+1/2,-1) = -h^{\alpha}_{A,0}(+1/2,-1/2,0) = +\frac{\sqrt{2}}{3}\frac{m_{\Lambda_b}-m_{\Lambda_c^*}}{\sqrt{q^2}}\sqrt{s_+}\eta^{*\alpha}(-1)\,, \quad \text{(C.28)}$$

$$-h^{\alpha}_{A,0}(+1/2,-1/2,+1) = \sqrt{2}h^{\alpha}_{A,0}(+1/2,+1/2,0) = +\frac{\sqrt{2}}{3}\frac{m_{\Lambda_b}-m_{\Lambda_c^*}}{\sqrt{q^2}}\sqrt{s_+}\eta^{*\alpha}(0)\,, \quad \text{(C.29)}$$

$$h^{\alpha}_{A,0}(-1/2,+1/2,-1) = -\sqrt{2}h^{\alpha}_{A,0}(-1/2,-1/2,0) = +\frac{\sqrt{2}}{3}\frac{m_{\Lambda_b}-m_{\Lambda_c^*}}{\sqrt{q^2}}\sqrt{s_+}\eta^{*\alpha}(0)\,. \quad \text{(C.30)}$$

JHEP06(2018)155

Using the above expressions, we can now list the helicity amplitudes for the transition $\Lambda_b \to \Lambda_c(2595)^+$. For the vector current we find the following non-zero helicity amplitudes:

$$+\mathcal{A}_V^{(1/2)}(+1/2,+1/2,0) = +\mathcal{A}_V^{(1/2)}(-1/2,-1/2,0) = -\sqrt{\frac{1}{3}} f_{1/2,0} \frac{m_{\Lambda_b}+m_{\Lambda_c^*}}{\sqrt{q^2}} \sqrt{4 m_{\Lambda_b} m_{\Lambda_c^*}}\,, \tag{C.31}$$

$$+\mathcal{A}_V^{(1/2)}(+1/2,+1/2,t) = +\mathcal{A}_V^{(1/2)}(-1/2,-1/2,t) = -\sqrt{\frac{1}{3}} f_{1/2,t} \frac{m_{\Lambda_b}-m_{\Lambda_c^*}}{\sqrt{q^2}} \sqrt{4 m_{\Lambda_b} m_{\Lambda_c^*}}\,, \tag{C.32}$$

$$+\mathcal{A}_V^{(1/2)}(+1/2,-1/2,-1) = +\mathcal{A}_V^{(1/2)}(-1/2,+1/2,+1) = -\sqrt{\frac{2}{3}} f_{1/2,\perp} \sqrt{4 m_{\Lambda_b} m_{\Lambda_c^*}}\,. \tag{C.33}$$

For the axialvector current we find similarly

$$+\mathcal{A}_A^{(1/2)}(+1/2,+1/2,0) = -\mathcal{A}_A^{(1/2)}(-1/2,-1/2,0) = -\sqrt{\frac{1}{3}} g_{1/2,0} \frac{m_{\Lambda_b}-m_{\Lambda_c^*}}{\sqrt{q^2}} \sqrt{4 m_{\Lambda_b} m_{\Lambda_c^*}}\,, \tag{C.34}$$

$$+\mathcal{A}_A^{(1/2)}(+1/2,+1/2,t) = -\mathcal{A}_A^{(1/2)}(-1/2,-1/2,t) = -\sqrt{\frac{1}{3}} g_{1/2,t} \frac{m_{\Lambda_b}+m_{\Lambda_c^*}}{\sqrt{q^2}} \sqrt{4 m_{\Lambda_b} m_{\Lambda_c^*}}\,, \tag{C.35}$$

$$+\mathcal{A}_A^{(1/2)}(+1/2,-1/2,-1) = -\mathcal{A}_A^{(1/2)}(-1/2,+1/2,+1) = +\sqrt{\frac{2}{3}} g_{1/2,\perp} \sqrt{4 m_{\Lambda_b} m_{\Lambda_c^*}}\,. \tag{C.36}$$

In the heavy quark expansion, if we use eq. (2.9) for the vector current, we calculated the following helicitity amplitudes:

$$\begin{aligned}
\mathcal{A}_V(+1/2,+1/2,0) &= +\mathcal{A}_V(-1/2,-1/2,0) \\
&= -\sqrt{\frac{1}{3}} \frac{m_{\Lambda_b}+m_{\Lambda_c^*}}{\sqrt{q^2}} \frac{\sqrt{s_+}}{m_{\Lambda_b} m_{\Lambda_c^*}} \left\{ \left[s_- \left(C_1(\bar{w}) + \frac{s_+ (C_2(\bar{w}) m_{\Lambda_c^*} + C_3(\bar{w}) m_{\Lambda_b})}{2 m_{\Lambda_b} m_{\Lambda_c^*} (m_{\Lambda_b}+m_{\Lambda_c^*})} \right) \right.\right. \\
&\quad + \frac{m_{\Lambda_b}-m_{\Lambda_c^*}}{m_{\Lambda_b}+m_{\Lambda_c^*}} \left(\frac{m_{\Lambda_b}^2 - m_{\Lambda_c^*}^2 + q^2}{2 m_{\Lambda_b}} \bar{\Lambda} - \frac{m_{\Lambda_b}^2 - m_{\Lambda_c^*}^2 - q^2}{2 m_{\Lambda_c^*}} \bar{\Lambda}' \right) \Bigg] \zeta \\
&\quad \left. -2(m_{\Lambda_b} - m_{\Lambda_c^*}) \zeta_{\rm SL} \right\},
\end{aligned} \tag{C.37}$$

$$\begin{aligned}
\mathcal{A}_V(+1/2,+1/2,t) &= +\mathcal{A}_V(-1/2,-1/2,t) = -\sqrt{\frac{1}{3}} \frac{m_{\Lambda_b}-m_{\Lambda_c^*}}{\sqrt{q^2}} \frac{\sqrt{s_-}}{m_{\Lambda_b} m_{\Lambda_c^*}} \left\{ \left[C_1(\bar{w}) s_+ \right.\right. \\
&\quad + \frac{m_{\Lambda_b}+m_{\Lambda_c^*}}{m_{\Lambda_b}-m_{\Lambda_c^*}} \left(\frac{m_{\Lambda_b}^2 - m_{\Lambda_c^*}^2 + q^2}{2 m_{\Lambda_b}} \left(\bar{\Lambda} + \frac{C_2(\bar{w}) s_+}{m_{\Lambda_b}+m_{\Lambda_c^*}} \right) \right. \\
&\quad \left. \left. - \frac{m_{\Lambda_b}^2 - m_{\Lambda_c^*}^2 - q^2}{2 m_{\Lambda_c^*}} \left(\bar{\Lambda}' - \frac{C_3(\bar{w}) s_+}{m_{\Lambda_b}+m_{\Lambda_c^*}} \right) \right) \right] \zeta - 2 \frac{(m_{\Lambda_b}+m_{\Lambda_c^*})^2}{m_{\Lambda_b}-m_{\Lambda_c^*}} \zeta_{\rm SL} \right\},
\end{aligned} \tag{C.38}$$

$$\begin{aligned}
\mathcal{A}_V(+1/2,-1/2,+1) &= +\mathcal{A}_V(-1/2,+1/2,-1) \\
&= -\sqrt{\frac{2}{3}} \frac{\sqrt{s_+}}{m_{\Lambda_b} m_{\Lambda_c^*}} \left\{ \left[C_1(\bar{w}) s_- + \frac{3 m_{\Lambda_b}^2 + m_{\Lambda_c^*}^2 - q^2}{2 m_{\Lambda_b}} \bar{\Lambda} \right.\right. \\
&\quad \left. \left. - \frac{m_{\Lambda_b}^2 + 3 m_{\Lambda_c^*}^2 - q^2}{2 m_{\Lambda_c^*}} \bar{\Lambda}' \right] \zeta - 2 m_{\Lambda_b} \zeta_{\rm SL} \right\},
\end{aligned} \tag{C.39}$$

while for the axial vector current in eq. (2.14) we obtain:

$$\begin{aligned}\mathcal{A}_A(+1/2,+1/2,0) &= -\mathcal{A}_A(-1/2,-1/2,0)\\ &= -\sqrt{\frac{1}{3}}\frac{m_{\Lambda_b}-m_{\Lambda_c^*}}{\sqrt{q^2}}\frac{\sqrt{s_-}}{m_{\Lambda_b}m_{\Lambda_c^*}}\left\{\left[s_+\left(C_1(\bar{w})-\frac{s_-(C_2(\bar{w})m_{\Lambda_c^*}+C_3(\bar{w})m_{\Lambda_b})}{2m_{\Lambda_b}m_{\Lambda_c^*}(m_{\Lambda_b}-m_{\Lambda_c^*})}\right)\right.\right.\\ &\quad +\frac{m_{\Lambda_b}+m_{\Lambda_c^*}}{m_{\Lambda_b}-m_{\Lambda_c^*}}\left(\frac{m_{\Lambda_b}^2-m_{\Lambda_c^*}^2+q^2}{2m_{\Lambda_b}}\bar{\Lambda}-\frac{m_{\Lambda_b}^2-m_{\Lambda_c^*}^2-q^2}{2m_{\Lambda_c^*}}\bar{\Lambda}'\right)\Bigg]\zeta\\ &\quad \left.-2(m_{\Lambda_b}+m_{\Lambda_c^*})\zeta_{\rm SL}\right\},\end{aligned} \tag{C.40}$$

$$\begin{aligned}\mathcal{A}_A(+1/2,+1/2,t) &= -\mathcal{A}_A(-1/2,-1/2,t) = -\sqrt{\frac{1}{3}}\frac{m_{\Lambda_b}+m_{\Lambda_c^*}}{\sqrt{q^2}}\frac{\sqrt{s_+}}{m_{\Lambda_b}m_{\Lambda_c^*}}\left\{\left[C_1(\bar{w})s_-\right.\right.\\ &\quad +\frac{m_{\Lambda_b}-m_{\Lambda_c^*}}{m_{\Lambda_b}+m_{\Lambda_c^*}}\left(\frac{m_{\Lambda_b}^2-m_{\Lambda_c^*}^2+q^2}{2m_{\Lambda_b}}\left(\bar{\Lambda}-\frac{C_2(\bar{w})s_+}{m_{\Lambda_b}-m_{\Lambda_c^*}}\right)\right.\\ &\quad \left.\left.-\frac{m_{\Lambda_b}^2-m_{\Lambda_c^*}^2-q^2}{2m_{\Lambda_c^*}}\left(\bar{\Lambda}'+\frac{C_3(\bar{w})s_+}{m_{\Lambda_b}+m_{\Lambda_c^*}}\right)\right)\right]\zeta-2\frac{(m_{\Lambda_b}-m_{\Lambda_c^*})^2}{m_{\Lambda_b}+m_{\Lambda_c^*}}\zeta_{\rm SL}\Bigg\},\end{aligned} \tag{C.41}$$

$$\begin{aligned}\mathcal{A}_A(+1/2,-1/2,+1) &= -\mathcal{A}_A(-1/2,+1/2,-1) = \sqrt{\frac{2}{3}}\frac{\sqrt{s_-}}{m_{\Lambda_b}m_{\Lambda_c^*}}\left\{\left[C_1(\bar{w})s_+\right.\right.\\ &\quad \left.\left.+\frac{3m_{\Lambda_b}^2+m_{\Lambda_c^*}^2-q^2}{2m_{\Lambda_b}}\bar{\Lambda}-\frac{m_{\Lambda_b}^2+3m_{\Lambda_c^*}^2-q^2}{2m_{\Lambda_c^*}}\bar{\Lambda}'\right]\zeta+2m_{\Lambda_b}\zeta_{\rm SL}\right\}.\end{aligned} \tag{C.42}$$

C.2 $1/2^+ \to 3/2^-$

We list here the $\Lambda_b \to \Lambda_c(2625)^+$ helicity amplitudes for various currents. For the scalar current

$$h_S^\alpha(s_b,s_c,\lambda_c) \equiv \bar{u}^\alpha(k,\eta(\lambda_c),s_c)u(p,s_b) \tag{C.43}$$

one finds the non-vanishing helicity amplitudes as follows:

$$\frac{\sqrt{2}}{3}h_S^\alpha(+1/2,+1/2,+1) = \sqrt{2}h_S^\alpha(-1/2,-1/2,+1) = h_S^\alpha(-1/2,+1/2,0) = \frac{\sqrt{2}}{3}\sqrt{s_+}\eta^{*\alpha}(+1)\,, \tag{C.44}$$

$$\frac{\sqrt{2}}{3}h_S^\alpha(-1/2,-1/2,-1) = \sqrt{2}h_S^\alpha(+1/2,+1/2,-1) = h_S^\alpha(+1/2,-1/2,0) = \frac{\sqrt{2}}{3}\sqrt{s_+}\eta^{*\alpha}(-1)\,, \tag{C.45}$$

$$h_S^\alpha(+1/2,-1/2,+1) = \frac{1}{\sqrt{2}}h_S^\alpha(+1/2,+1/2,0) = \frac{\sqrt{2}}{3}\sqrt{s_+}\eta^{*\alpha}(0)\,, \tag{C.46}$$

$$h_S^\alpha(-1/2,+1/2,-1) = \frac{1}{\sqrt{2}}h_S^\alpha(-1/2,-1/2,0) = \frac{\sqrt{2}}{3}\sqrt{s_+}\eta^{*\alpha}(0)\,. \tag{C.47}$$

For the pseudoscalar current

$$h_P^\alpha(s_b,s_c,\lambda_c) \equiv \bar{u}^\alpha(k,\eta(\lambda_c),s_c)\gamma_5 u(p,s_b) \tag{C.48}$$

JHEP06(2018)155

one finds similarly:

$$-\frac{\sqrt{2}}{3}h_P^\alpha(+1/2,+1/2,+1)=\sqrt{2}h_P^\alpha(-1/2,-1/2,+1)=h_P^\alpha(-1/2,+1/2,0)=+\frac{\sqrt{2}}{3}\sqrt{s_-}\eta^{*\alpha}(+1)\,, \tag{C.49}$$

$$-\frac{\sqrt{2}}{3}h_P^\alpha(-1/2,-1/2,-1)=\sqrt{2}h_P^\alpha(+1/2,+1/2,-1)=h_P^\alpha(+1/2,-1/2,0)=-\frac{\sqrt{2}}{3}\sqrt{s_-}\eta^{*\alpha}(-1)\,, \tag{C.50}$$

$$h_P^\alpha(+1/2,-1/2,+1)=\frac{1}{\sqrt{2}}h_P^\alpha(+1/2,+1/2,0)=-\frac{\sqrt{2}}{3}\sqrt{s_-}\eta^{*\alpha}(0)\,, \tag{C.51}$$

$$h_P^\alpha(-1/2,+1/2,-1)=\frac{1}{\sqrt{2}}h_P^\alpha(-1/2,-1/2,0)=+\frac{\sqrt{2}}{3}\sqrt{s_-}\eta^{*\alpha}(0)\,. \tag{C.52}$$

For the vector current we investigate

$$h^\alpha_{V,\lambda_q}(s_b,s_c,\lambda_c)\equiv\bar{u}^\alpha(k,\eta(\lambda_c),s_c)\not{\epsilon}^*(\lambda_q)u(p,s_b)\,, \tag{C.53}$$

and identify

$$h^\alpha_{V,t}(s_b,s_c,\lambda_c)=\frac{m_{\Lambda_b}-m_{\Lambda_c^*}}{\sqrt{q^2}}h^\alpha_S(s_b,s_c,\lambda_c)\,. \tag{C.54}$$

For the transverse polarisations we find:

$$\begin{aligned}-\frac{\sqrt{2}}{3}h^\alpha_{V,+1}(-1/2,+1/2,+1)&=\sqrt{2}h^\alpha_{V,-1}(+1/2,-1/2,+1)\\&=h^\alpha_{V,-1}(+1/2,+1/2,0)=-\frac{2}{3}\sqrt{s_-}\eta^{*\alpha}(+1)\,,\end{aligned} \tag{C.55}$$

$$\begin{aligned}\frac{\sqrt{2}}{3}h^\alpha_{V,-1}(+1/2,-1/2,-1)&=\sqrt{2}h^\alpha_{V,+1}(-1/2,+1/2,-1)\\&=h^\alpha_{V,+1}(-1/2,-1/2,0)=-\frac{2}{3}\sqrt{s_-}\eta^{*\alpha}(-1)\,,\end{aligned} \tag{C.56}$$

$$h^\alpha_{V,+1}(-1/2,-1/2,+1)=\frac{1}{\sqrt{2}}h^\alpha_{V,+1}(-1/2,+1/2,0)=-\frac{2}{3}\sqrt{s_-}\eta^{*\alpha}(0)\,, \tag{C.57}$$

$$h^\alpha_{V,-1}(+1/2,+1/2,-1)=\frac{1}{\sqrt{2}}h^\alpha_{V,-1}(+1/2,-1/2,0)=-\frac{2}{3}\sqrt{s_-}\eta^{*\alpha}(0)\,. \tag{C.58}$$

For the longitudinal polarisation we find

$$\begin{aligned}\frac{\sqrt{2}}{3}h^\alpha_{V,0}(+1/2,+1/2,+1)&=\sqrt{2}h^\alpha_{V,0}(-1/2,-1/2,+1)\\&=h^\alpha_{V,0}(-1/2,+1/2,0)=\frac{\sqrt{2}}{3}\frac{m_{\Lambda_b}+m_{\Lambda_c^*}}{\sqrt{q^2}}\sqrt{s_-}\eta^{*\alpha}(+1)\,,\end{aligned} \tag{C.59}$$

$$\begin{aligned}\frac{\sqrt{2}}{3}h^\alpha_{V,0}(-1/2,-1/2,-1)&=\sqrt{2}h^\alpha_{V,0}(+1/2,+1/2,-1)\\&=h^\alpha_{V,0}(+1/2,-1/2,0)=\frac{\sqrt{2}}{3}\frac{m_{\Lambda_b}+m_{\Lambda_c^*}}{\sqrt{q^2}}\sqrt{s_-}\eta^{*\alpha}(-1)\,,\end{aligned} \tag{C.60}$$

$$h^\alpha_{V,0}(+1/2,-1/2,+1)=\frac{1}{\sqrt{2}}h^\alpha_{V,0}(+1/2,+1/2,0)=\frac{\sqrt{2}}{3}\frac{m_{\Lambda_b}+m_{\Lambda_c^*}}{\sqrt{q^2}}\sqrt{s_-}\eta^{*\alpha}(0)\,, \tag{C.61}$$

$$h^\alpha_{V,0}(-1/2,+1/2,-1)=\frac{1}{\sqrt{2}}h^\alpha_{V,0}(-1/2,-1/2,0)=\frac{\sqrt{2}}{3}\frac{m_{\Lambda_b}+m_{\Lambda_c^*}}{\sqrt{q^2}}\sqrt{s_-}\eta^{*\alpha}(0)\,. \tag{C.62}$$

JHEP06(2018)155

For the axialvector current we investigate

$$h^{\alpha}_{A,\lambda_q}(s_b,s_c,\lambda_c) \equiv \bar{u}^{\alpha}(k,\eta(\lambda_c),s_c)\not{\epsilon}^{*}(\lambda_q)\gamma_5 u(p,s_b)\,, \tag{C.63}$$

and identify

$$h^{\alpha}_{A,t}(s_b,s_c,\lambda_c) = -\frac{m_{\Lambda_b}+m_{\Lambda_c^*}}{\sqrt{q^2}} h^{\alpha}_{P}(s_b,s_c,\lambda_c)\,. \tag{C.64}$$

For the transverse polarisations we find:

$$\begin{aligned}
-\frac{\sqrt{2}}{3}h^{\alpha}_{A,+1}(-1/2,+1/2,+1) &= \sqrt{2}h^{\alpha}_{A,-1}(+1/2,-1/2,+1) \\
&= h^{\alpha}_{A,-1}(+1/2,+1/2,0) = +\frac{2}{3}\sqrt{s_+}\eta^{*\alpha}(+1)\,, \qquad \text{(C.65)}\\
-\frac{\sqrt{2}}{3}h^{\alpha}_{A,-1}(+1/2,-1/2,-1) &= \sqrt{2}h^{\alpha}_{A,+1}(-1/2,+1/2,-1) \\
&= h^{\alpha}_{A,+1}(-1/2,-1/2,0) = -\frac{2}{3}\sqrt{s_+}\eta^{*\alpha}(-1)\,, \qquad \text{(C.66)}\\
h^{\alpha}_{A,+1}(-1/2,-1/2,+1) &= \frac{1}{\sqrt{2}}h^{\alpha}_{A,+1}(-1/2,+1/2,0) = -\frac{2}{3}\sqrt{s_+}\eta^{*\alpha}(0)\,, \qquad \text{(C.67)}\\
h^{\alpha}_{A,-1}(+1/2,+1/2,-1) &= \frac{1}{\sqrt{2}}h^{\alpha}_{A,-1}(+1/2,-1/2,0) = +\frac{2}{3}\sqrt{s_+}\eta^{*\alpha}(0)\,. \qquad \text{(C.68)}
\end{aligned}$$

For the longitudinal polarisation we find

$$\begin{aligned}
-\frac{\sqrt{2}}{3}h^{\alpha}_{A,0}(+1/2,+1/2,+1) &= \sqrt{2}h^{\alpha}_{A,0}(-1/2,-1/2,+1) \\
&= h^{\alpha}_{A,0}(-1/2,+1/2,0) = -\frac{\sqrt{2}}{3}\frac{m_{\Lambda_b}-m_{\Lambda_c^*}}{\sqrt{q^2}}\sqrt{s_+}\eta^{*\alpha}(+1)\,, \qquad \text{(C.69)}\\
-\frac{\sqrt{2}}{3}h^{\alpha}_{A,0}(-1/2,-1/2,-1) &= \sqrt{2}h^{\alpha}_{A,0}(+1/2,+1/2,-1) \\
&= h^{\alpha}_{A,0}(+1/2,-1/2,0) = +\frac{\sqrt{2}}{3}\frac{m_{\Lambda_b}-m_{\Lambda_c^*}}{\sqrt{q^2}}\sqrt{s_+}\eta^{*\alpha}(-1)\,, \qquad \text{(C.70)}\\
h^{\alpha}_{A,0}(+1/2,-1/2,+1) &= \frac{1}{\sqrt{2}}h^{\alpha}_{A,0}(+1/2,+1/2,0) = +\frac{\sqrt{2}}{3}\frac{m_{\Lambda_b}-m_{\Lambda_c^*}}{\sqrt{q^2}}\sqrt{s_+}\eta^{*\alpha}(0)\,, \qquad \text{(C.71)}\\
h^{\alpha}_{A,0}(-1/2,+1/2,-1) &= \frac{1}{\sqrt{2}}h^{\alpha}_{A,0}(-1/2,-1/2,0) = -\frac{\sqrt{2}}{3}\frac{m_{\Lambda_b}-m_{\Lambda_c^*}}{\sqrt{q^2}}\sqrt{s_+}\eta^{*\alpha}(0)\,. \qquad \text{(C.72)}
\end{aligned}$$

JHEP06(2018)155

For the vector current we find the following non-zero helicity amplitudes:

$$+\mathcal{A}_V^{(3/2)}(+1/2,+3/2,+1) = +\mathcal{A}_V^{(3/2)}(-1/2,-3/2,-1) = -2F_{3/2,\perp}\sqrt{4\,m_{\Lambda_b}\,m_{\Lambda_c^*}}\,, \tag{C.73}$$

$$+\mathcal{A}_V^{(3/2)}(+1/2,+1/2,0) = +\mathcal{A}_V^{(3/2)}(-1/2,-1/2,0) = +\sqrt{\frac{2}{3}}F_{1/2,0}\frac{m_{\Lambda_b}+m_{\Lambda_c^*}}{\sqrt{q^2}}\sqrt{4\,m_{\Lambda_b}\,m_{\Lambda_c^*}}\,, \tag{C.74}$$

$$+\mathcal{A}_V^{(3/2)}(+1/2,+1/2,t) = +\mathcal{A}_V^{(3/2)}(-1/2,-1/2,t) = +\sqrt{\frac{2}{3}}F_{1/2,t}\frac{m_{\Lambda_b}-m_{\Lambda_c^*}}{\sqrt{q^2}}\sqrt{4\,m_{\Lambda_b}\,m_{\Lambda_c^*}}\,, \tag{C.75}$$

$$+\mathcal{A}_V^{(3/2)}(+1/2,-1/2,-1) = +\mathcal{A}_V^{(3/2)}(-1/2,+1/2,+1) = -\frac{2}{\sqrt{3}}F_{1/2,\perp}\sqrt{4\,m_{\Lambda_b}\,m_{\Lambda_c^*}}\,. \tag{C.76}$$

For the axialvector current we find similarly

$$+\mathcal{A}_A^{(3/2)}(+1/2,+3/2,+1) = -\mathcal{A}_A^{(3/2)}(-1/2,-3/2,-1) = -2G_{3/2,\perp}\sqrt{4\,m_{\Lambda_b}\,m_{\Lambda_c^*}}\,, \tag{C.77}$$

$$+\mathcal{A}_A^{(3/2)}(+1/2,+1/2,0) = -\mathcal{A}_A^{(3/2)}(-1/2,-1/2,0) = +\sqrt{\frac{2}{3}}G_{1/2,0}\frac{m_{\Lambda_b}-m_{\Lambda_c^*}}{\sqrt{q^2}}\sqrt{4\,m_{\Lambda_b}\,m_{\Lambda_c^*}}\,, \tag{C.78}$$

$$+\mathcal{A}_A^{(3/2)}(+1/2,+1/2,t) = -\mathcal{A}_A^{(3/2)}(-1/2,-1/2,t) = +\sqrt{\frac{2}{3}}G_{1/2,t}\frac{m_{\Lambda_b}+m_{\Lambda_c^*}}{\sqrt{q^2}}\sqrt{4\,m_{\Lambda_b}\,m_{\Lambda_c^*}}\,, \tag{C.79}$$

$$+\mathcal{A}_A^{(3/2)}(+1/2,-1/2,-1) = -\mathcal{A}_A^{(3/2)}(-1/2,+1/2,+1) = +\frac{2}{\sqrt{3}}G_{1/2,\perp}\sqrt{4\,m_{\Lambda_b}\,m_{\Lambda_c^*}}\,. \tag{C.80}$$

In the heavy quark expansion, the helicity amplitudes related to the vector current eq. (2.9) read

$$\mathcal{A}_V(+1/2,+3/2,+1) = +\mathcal{A}_V(-1/2,-3/2,-1) = +2\frac{\sqrt{s_+}}{m_{\Lambda_b}}\zeta_{\rm SL}\,, \tag{C.81}$$

$$\begin{aligned}\mathcal{A}_V(+1/2,+1/2,0) &= +\mathcal{A}_V(-1/2,-1/2,0)\\ &= +\sqrt{\frac{2}{3}}\frac{m_{\Lambda_b}+m_{\Lambda_c^*}}{\sqrt{q^2}}\frac{\sqrt{s_+}}{m_{\Lambda_b}m_{\Lambda_c^*}}\left\{\left[s_-\left(C_1(\bar w)+\frac{s_+(C_2(\bar w)m_{\Lambda_c^*}+C_3(\bar w)m_{\Lambda_b})}{2m_{\Lambda_b}m_{\Lambda_c^*}(m_{\Lambda_b}+m_{\Lambda_c^*})}\right)\right.\right.\\ &\quad\left.+\frac{m_{\Lambda_b}-m_{\Lambda_c^*}}{m_{\Lambda_b}+m_{\Lambda_c^*}}\left(\frac{m_{\Lambda_b}^2-m_{\Lambda_c^*}^2+q^2}{2m_{\Lambda_b}}\bar\Lambda-\frac{m_{\Lambda_b}^2-m_{\Lambda_c^*}^2-q^2}{2m_{\Lambda_c^*}}\bar\Lambda'\right)\right]\zeta\\ &\quad\left.+(m_{\Lambda_b}-m_{\Lambda_c^*})\zeta_{\rm SL}\right\},\end{aligned} \tag{C.82}$$

$$\begin{aligned}\mathcal{A}_V(+1/2,+1/2,t) &= +\mathcal{A}_V(-1/2,-1/2,t) = +\sqrt{\frac{2}{3}}\frac{m_{\Lambda_b}-m_{\Lambda_c^*}}{m_{\Lambda_b}m_{\Lambda_c^*}}\frac{\sqrt{s_-}}{\sqrt{q^2}}\left\{\left[s_+\right.\right.\\ &\quad+\frac{m_{\Lambda_b}+m_{\Lambda_c^*}}{m_{\Lambda_b}-m_{\Lambda_c^*}}\left(\frac{m_{\Lambda_b}^2-m_{\Lambda_c^*}^2+q^2}{2m_{\Lambda_b}}\left(\bar\Lambda+\frac{C_2(\bar w)s_+}{m_{\Lambda_b}+m_{\Lambda_c^*}}\right)\right.\\ &\quad\left.\left.-\frac{m_{\Lambda_b}^2-m_{\Lambda_c^*}^2-q^2}{2m_{\Lambda_c^*}}\left(\bar\Lambda'-\frac{C_3(\bar w)s_+}{m_{\Lambda_b}+m_{\Lambda_c^*}}\right)\right)\right]\zeta\\ &\quad\left.+\frac{(m_{\Lambda_b}+m_{\Lambda_c^*})^2}{m_{\Lambda_b}-m_{\Lambda_c^*}}\zeta_{\rm SL}\right\},\end{aligned} \tag{C.83}$$

$$\begin{aligned}\mathcal{A}_V(+1/2,-1/2,-1) &= +\mathcal{A}_V(-1/2,+1/2,+1) = -\sqrt{\frac{4}{3}}\frac{\sqrt{s_+}}{m_{\Lambda_b}m_{\Lambda_c^*}}\left\{\left[s_-C_1(\bar w)-\frac{3m_{\Lambda_b}^2+m_{\Lambda_c^*}^2-q^2}{2m_{\Lambda_b}}\bar\Lambda\right.\right.\\ &\quad\left.\left.+\frac{m_{\Lambda_b}^2+3m_{\Lambda_c^*}^2-q^2}{2m_{\Lambda_c^*}}\bar\Lambda'\right]\zeta+m_{\Lambda_b}\zeta_{\rm SL}\right\},\end{aligned} \tag{C.84}$$

JHEP06(2018)155

while for the axial vector current eq. (2.14), we obtain

$$\mathcal{A}_A(+1/2,+3/2,-1) = -\mathcal{A}_A(-1/2,-3/2,+1) = 2\frac{\sqrt{s_-}}{m_{\Lambda_b}}\zeta_{\rm SL}\,, \tag{C.85}$$

$$\begin{aligned}\mathcal{A}_A(+1/2,+1/2,0) &= -\mathcal{A}_A(-1/2,-1/2,0)\\ &= +\sqrt{\frac{2}{3}}\frac{m_{\Lambda_b}-m_{\Lambda_c^*}}{\sqrt{q^2}}\frac{\sqrt{s_-}}{m_{\Lambda_b}m_{\Lambda_c^*}}\left\{\left[s_+\left(C_1(\bar{w})-\frac{s_-(C_2(\bar{w})m_{\Lambda_c^*}+C_3(\bar{w})m_{\Lambda_b})}{2m_{\Lambda_b}m_{\Lambda_c^*}(m_{\Lambda_b}+m_{\Lambda_c^*})}\right)\right.\right.\\ &\quad+\left(\frac{m_{\Lambda_b}^2-m_{\Lambda_c^*}^2+q^2}{2m_{\Lambda_b}}\bar{\Lambda}-\frac{m_{\Lambda_b}^2-m_{\Lambda_c^*}^2-q^2}{2m_{\Lambda_c^*}}\bar{\Lambda}'\right)\frac{(m_{\Lambda_b}+m_{\Lambda_c^*})}{m_{\Lambda_b}-m_{\Lambda_c^*}}\Bigg]\zeta\\ &\quad\left.+(m_{\Lambda_b}+m_{\Lambda_c^*})\zeta_{\rm SL}\right\},\end{aligned} \tag{C.86}$$

$$\begin{aligned}\mathcal{A}_A(+1/2,+1/2,t) &= -\mathcal{A}_A(-1/2,-1/2,t) = +\sqrt{\frac{2}{3}}\frac{m_{\Lambda_b}+m_{\Lambda_c^*}}{\sqrt{q^2}}\frac{\sqrt{s_+}}{m_{\Lambda_b}m_{\Lambda_c^*}}\left\{\left[s_-\right.\right.\\ &\quad+\left(\frac{m_{\Lambda_b}^2-m_{\Lambda_c^*}^2+q^2}{2m_{\Lambda_b}}\left(\bar{\Lambda}-\frac{C_2(\bar{w})s_-}{m_{\Lambda_b}-m_{\Lambda_c^*}}\right)-\frac{m_{\Lambda_b}^2-m_{\Lambda_c^*}^2-q^2}{2m_{\Lambda_c^*}}\left(\bar{\Lambda}'+\frac{C_3(\bar{w})s_-}{m_{\Lambda_b}-m_{\Lambda_c^*}}\right)\right)\\ &\quad\left.\times\frac{(m_{\Lambda_b}-m_{\Lambda_c^*})}{m_{\Lambda_b}+m_{\Lambda_c^*}}\right]\zeta+\frac{(m_{\Lambda_b}-m_{\Lambda_c^*})^2}{m_{\Lambda_b}+m_{\Lambda_c^*}}\zeta_{\rm SL}\Bigg\},\end{aligned} \tag{C.87}$$

$$\begin{aligned}\mathcal{A}_A(+1/2,-1/2,+1) &= -\mathcal{A}_A(-1/2,+1/2,-1) = +\sqrt{\frac{4}{3}}\frac{\sqrt{s_-}}{m_{\Lambda_b}m_{\Lambda_c^*}}\left\{\left[s_+C_1(\bar{w})+\frac{3m_{\Lambda_b}^2+m_{\Lambda_c^*}^2-q^2}{2m_{\Lambda_b}}\bar{\Lambda}\right.\right.\\ &\quad\left.\left.-\frac{m_{\Lambda_b}^2+3m_{\Lambda_c^*}^2-q^2}{2m_{\Lambda_c^*}}\bar{\Lambda}'\right]\zeta+m_{\Lambda_b}\zeta_{\rm SL}\right\}.\end{aligned} \tag{C.88}$$

D Details on the kinematics

We choose the z axis along the flight direction of the Λ_c^*. Thus, in the rest frame of the Λ_b^0 (B-RF) one has

$$p^\mu\big|_{\text{B-RF}} = (m_{\Lambda_b^0},0,0,0)\,, \tag{D.1}$$

$$q^\mu\big|_{\text{B-RF}} = (q^0,0,0,-|\vec{q}|)\,, \tag{D.2}$$

$$k^\mu\big|_{\text{B-RF}} = (m_{\Lambda_b^0}-q^0,0,0,+|\vec{q}|)\,. \tag{D.3}$$

We chose to describe the decay through the invariants q^2 and obtain

$$q^0\big|_{B-RF} = \frac{m_{\Lambda_b}^2-m_{\Lambda_c^*}^2+q^2}{2m_{\Lambda_b}}\,,\qquad |\vec{q}|\big|_{B-RF} = \frac{\sqrt{\lambda(m_{\Lambda_b}^2,m_{\Lambda_c^*}^2,q^2)}}{2m_{\Lambda_b}}\,, \tag{D.4}$$

where λ is the usual Källén function.

JHEP06(2018)155

The description of the Λ_c^* involves a spin-1 polarisation vector $\eta(m)$ along the positive z direction. According to [38] we can use

$$\eta(\pm)|_{B-RF} = (0, \mp 1, -i, 0)/\sqrt{2}\,, \tag{D.5}$$
$$\eta(0)|_{B-RF} = (|\vec{q}|, 0, 0, m_{\Lambda_b} - q^0)/m_{\Lambda_c^*}\,. \tag{D.6}$$

In order to facilitate the calculation we introduce artificial polarisation vectors $\varepsilon(n)$ which fulfill the following relations:

$$\varepsilon(n) \cdot q = 0 \qquad n = \pm, 0 \tag{D.7}$$
$$\varepsilon(n) \cdot \varepsilon^\dagger(n') = g_{nn'} \qquad g_{nn'} = \mathrm{diag}(+,-,-,-) \text{ for } n, n' = t, +, -, 0 \tag{D.8}$$
$$\varepsilon(n)_\mu \varepsilon^\dagger(n')_\nu g_{nn'} = g_{\mu\nu}\,. \tag{D.9}$$

Within the $\ell\nu$ rest frame these relations are fulfilled by the set

$$\varepsilon^\mu(t)\big|_{\ell\nu-RF} = (1, 0, 0, 0)\,, \tag{D.10}$$
$$\varepsilon^\mu(\pm)\big|_{\ell\nu-RF} = (0, \pm 1, -i, 0)/\sqrt{2}\,, \tag{D.11}$$
$$\varepsilon^\mu(0)\big|_{\ell\nu-RF} = (0, 0, 0, -1)\,. \tag{D.12}$$

Using a boost along z, one obtains in the B rest frame

$$\varepsilon^\mu(t)\big|_{B-RF} = (q^0, 0, 0, -|\vec{q}|)/\sqrt{q^2} = q^\mu/\sqrt{q^2}\,, \tag{D.13}$$
$$\varepsilon^\mu(0)\big|_{B-RF} = (+|\vec{q}|, 0, 0, -q_0)/\sqrt{q^2}\,, \tag{D.14}$$

while the $\varepsilon(\pm)$ remain invariant under that boost. Comments are due on the choice of the polarisation vectors, especially the signs of $\varepsilon^z(0)$ as well as $\varepsilon^y(\pm)$. These haven been adopted to obtain longitudinal and right-handed/left-handed polarisation of the $\ell\nu$ system, which moves along the *negative* z-axis. The phase convention is as in [38].

E Explicit spinor representations

In the course of the calculations we need to use explicit representations of spinors for an arbitrary momentum and fixed helicity in their rest frame. In the chiral representation of Dirac spinors, one obtains for a u spinor with momentum p^μ,

$$p^\mu = (p^0, |\vec{p}|\sin\theta\cos\phi, |\vec{p}|\sin\theta\sin\phi, |\vec{p}|\cos\theta), \tag{E.1}$$

JHEP06(2018)155

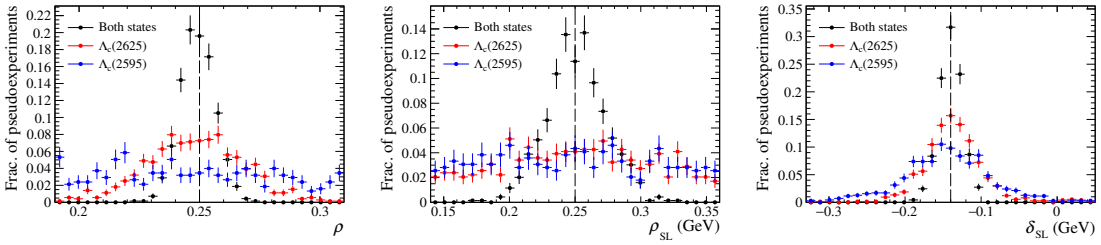

Figure 5. Distribution of the Isgur-Wise parameters as fitted from an ensemble of pseudo-experiments. The distributions are shown for the cases when one of the two Λ_c^{*+} states is fitted, as well as the combination of both. Both q^2 and $\cos\theta_l$ are fitted simultaneously.

with $p^2 = m^2$ and helicity $h = \pm 1/2$ in their respective rest frames [38]

$$u(p, h = +1/2) = \frac{\gamma^0}{\sqrt{2(p^0 + m)}} \begin{bmatrix} +(p^0 + m - |\vec{p}|)\ \cos(\theta/2) \\ +(p^0 + m - |\vec{p}|)\ \sin(\theta/2)\ \exp(+i\phi) \\ +(p^0 + m + |\vec{p}|)\ \cos(\theta/2) \\ +(p^0 + m + |\vec{p}|)\ \sin(\theta/2)\ \exp(+i\phi) \end{bmatrix} \tag{E.2}$$

$$u(p, h = -1/2) = \frac{\gamma^0}{\sqrt{2(p^0 + m)}} \begin{bmatrix} -(p^0 + m + |\vec{p}|)\ \sin(\theta/2)\ \exp(-i\phi) \\ +(p^0 + m + |\vec{p}|)\ \cos(\theta/2) \\ -(p^0 + m - |\vec{p}|)\ \sin(\theta/2)\ \exp(-i\phi) \\ +(p^0 + m - |\vec{p}|)\ \cos(\theta/2) \end{bmatrix} . \tag{E.3}$$

F Formulae

For the Levi-Civita tensor we use the convention

$$\varepsilon^{0123} = -\varepsilon_{0123} = +1\,. \tag{F.1}$$

In this convention one has

$$\mathrm{Tr}\,\gamma^\mu\gamma^\nu\gamma^\rho\gamma^\sigma\gamma_5 = -4i\varepsilon^{\mu\nu\rho\sigma} \tag{F.2}$$

$$\varepsilon^{\alpha\beta\mu\nu}\varepsilon_{\alpha\beta\rho\sigma} = -2(\delta^\mu_\rho\delta^\nu_\sigma - \delta^\mu_\sigma\delta^\nu_\rho) \tag{F.3}$$

$$\sigma_{\mu\nu}\gamma_5 = \frac{i}{2}\varepsilon_{\mu\nu\alpha\beta}\sigma^{\alpha\beta} \tag{F.4}$$

G Additional material on the sensitivity study

We show in figure 5 the distributions of the Isgur-Wise parameters resulting from a two-dimensional fit to both q^2 and $\cos\theta_l$, comparing ensembles of pseudo-experiments using only the $\Lambda_c(2595)^+$, only the $\Lambda_c(2625)^+$, or both. In figure 6 we investigate the correlations between the Isgur-Wise parameters resulting from a two-dimensional fit to q^2 and $\cos\theta_l$ of the three sets of pseudo-experiments. In particular, the leftmost plots demonstrate how only a simultaneous fit to both Λ_c^{*+} states can solve the degeneracy between the two slope parameters. Moreover, both $\Lambda_c(2595)^+$ and $\Lambda_c(2625)^+$ data sets are individually sensitive to the δ_{SL} parameter, but a simultaneous fit provides much better precision.

JHEP06(2018)155

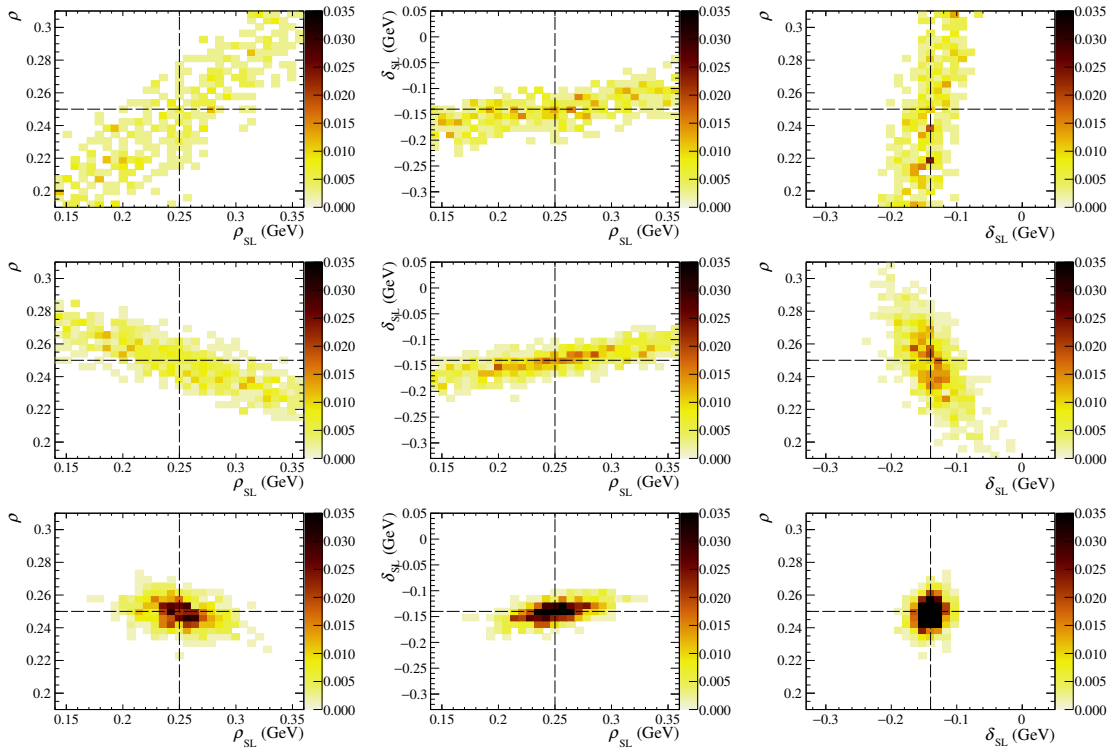

Figure 6. Two-dimensional distributions of the Isgur-Wise parameters as fitted from an ensemble of pseudoexperiments. Both q^2 and $\cos\theta_l$ are fitted simultaneously. Only simulated $\Lambda_c(2595)^+$ and $\Lambda_c(2625)^+$ data are used for the pseudoexperiments shown in the first and second row, respectively. Both states are fitted in the pseudoexperiments shown in the third row. The dashed lines indicate the numerical values of the parameters used to generate the pseudoexperiments.

References

[1] BaBar collaboration, J.P. Lees et al., *Evidence for an excess of* $\bar{B} \to D^{(*)}\tau^-\bar{\nu}_\tau$ *decays*, *Phys. Rev. Lett.* **109** (2012) 101802 [arXiv:1205.5442] [INSPIRE].

[2] BaBar collaboration, J.P. Lees et al., *Measurement of an Excess of* $\bar{B} \to D^{(*)}\tau^-\bar{\nu}_\tau$ *Decays and Implications for Charged Higgs Bosons*, *Phys. Rev.* **D 88** (2013) 072012 [arXiv:1303.0571] [INSPIRE].

[3] Belle collaboration, M. Huschle et al., *Measurement of the branching ratio of* $\bar{B} \to D^{(*)}\tau^-\bar{\nu}_\tau$ *relative to* $\bar{B} \to D^{(*)}\ell^-\bar{\nu}_\ell$ *decays with hadronic tagging at Belle*, *Phys. Rev.* **D 92** (2015) 072014 [arXiv:1507.03233] [INSPIRE].

[4] LHCb collaboration, *Measurement of the ratio of branching fractions* $\mathcal{B}(\bar{B}^0 \to D^{*+}\tau^-\bar{\nu}_\tau)/\mathcal{B}(\bar{B}^0 \to D^{*+}\mu^-\bar{\nu}_\mu)$, *Phys. Rev. Lett.* **115** (2015) 111803 [*Erratum ibid.* **115** (2015) 159901] [arXiv:1506.08614] [INSPIRE].

JHEP06(2018)155

[5] Belle collaboration, Y. Sato et al., *Measurement of the branching ratio of $\bar{B}^0 \to D^{*+}\tau^-\bar{\nu}_\tau$ relative to $\bar{B}^0 \to D^{*+}\ell^-\bar{\nu}_\ell$ decays with a semileptonic tagging method*, *Phys. Rev.* **D 94** (2016) 072007 [arXiv:1607.07923] [INSPIRE].

[6] Belle collaboration, S. Hirose et al., *Measurement of the τ lepton polarization and $R(D^*)$ in the decay $\bar{B} \to D^*\tau^-\bar{\nu}_\tau$*, *Phys. Rev. Lett.* **118** (2017) 211801 [arXiv:1612.00529] [INSPIRE].

[7] LHCb collaboration, *Measurement of the ratio of the $B^0 \to D^{*-}\tau^+\nu_\tau$ and $B^0 \to D^{*-}\mu^+\nu_\mu$ branching fractions using three-prong τ-lepton decays*, *Phys. Rev. Lett.* **120** (2018) 171802 [arXiv:1708.08856] [INSPIRE].

[8] LHCb collaboration, *Test of Lepton Flavor Universality by the measurement of the $B^0 \to D^{*-}\tau^+\nu_\tau$ branching fraction using three-prong τ decays*, *Phys. Rev.* **D 97** (2018) 072013 [arXiv:1711.02505] [INSPIRE].

[9] LHCb collaboration, *Measurement of the ratio of branching fractions $\mathcal{B}(B_c^+ \to J/\psi\tau^+\nu_\tau)/\mathcal{B}(B_c^+ \to J/\psi\mu^+\nu_\mu)$*, *Phys. Rev. Lett.* **120** (2018) 121801 [arXiv:1711.05623] [INSPIRE].

[10] LHCb collaboration, *Test of lepton universality using $B^+ \to K^+\ell^+\ell^-$ decays*, *Phys. Rev. Lett.* **113** (2014) 151601 [arXiv:1406.6482] [INSPIRE].

[11] LHCb collaboration, *Test of lepton universality with $B^0 \to K^{*0}\ell^+\ell^-$ decays*, *JHEP* **08** (2017) 055 [arXiv:1705.05802] [INSPIRE].

[12] LHCb collaboration, *Measurement of b-hadron production fractions in 7 TeV pp collisions*, *Phys. Rev.* **D 85** (2012) 032008 [arXiv:1111.2357] [INSPIRE].

[13] LHCb collaboration, *Study of the kinematic dependences of Λ_b^0 production in pp collisions and a measurement of the $\Lambda_b^0 \to \Lambda_c^+ \pi^-$ branching fraction*, *JHEP* **08** (2014) 143 [arXiv:1405.6842] [INSPIRE].

[14] W. Detmold, C. Lehner and S. Meinel, *$\Lambda_b \to p\ell^-\bar{\nu}_\ell$ and $\Lambda_b \to \Lambda_c\ell^-\bar{\nu}_\ell$ form factors from lattice QCD with relativistic heavy quarks*, *Phys. Rev.* **D 92** (2015) 034503 [arXiv:1503.01421] [INSPIRE].

[15] A. Datta, S. Kamali, S. Meinel and A. Rashed, *Phenomenology of $\Lambda_b \to \Lambda_c\tau\overline{\nu}_\tau$ using lattice QCD calculations*, *JHEP* **08** (2017) 131 [arXiv:1702.02243] [INSPIRE].

[16] LHCb collaboration, *Measurement of the shape of the $\Lambda_b^0 \to \Lambda_c^+\mu^-\overline{\nu}_\mu$ differential decay rate*, *Phys. Rev.* **D 96** (2017) 112005 [arXiv:1709.01920] [INSPIRE].

[17] A.F. Falk, *Hadrons of arbitrary spin in the heavy quark effective theory*, *Nucl. Phys.* **B 378** (1992) 79 [INSPIRE].

[18] A.K. Leibovich and I.W. Stewart, *Semileptonic Λ_b decay to excited Λ_c baryons at order Λ_{QCD}/m_Q*, *Phys. Rev.* **D 57** (1998) 5620 [hep-ph/9711257] [INSPIRE].

[19] S. Meinel and G. Rendon, *Lattice QCD calculation of form factors for $\Lambda_b \to \Lambda(1520)\ell^+\ell^-$ decays*, PoS(LATTICE2016)299 [arXiv:1608.08110] [INSPIRE].

[20] T. Feldmann and M.W.Y. Yip, *Form Factors for $\Lambda_b \to \Lambda$ Transitions in SCET*, *Phys. Rev.* **D 85** (2012) 014035 [*Erratum ibid.* **D 86** (2012) 079901] [arXiv:1111.1844] [INSPIRE].

[21] M. Neubert, *Heavy quark symmetry*, *Phys. Rept.* **245** (1994) 259 [hep-ph/9306320] [INSPIRE].

[22] E.E. Jenkins, A.V. Manohar and M.B. Wise, *The Baryon Isgur-Wise function in the large N_c limit*, *Nucl. Phys.* **B 396** (1993) 38 [hep-ph/9208248] [INSPIRE].

JHEP06(2018)155

[23] A.V. Manohar and M.B. Wise, *Heavy quark physics*, *Camb. Monogr. Part. Phys. Nucl. Phys. Cosmol.* **10** (2000) 1 [INSPIRE].

[24] M.A. Shifman, N.G. Uraltsev and A.I. Vainshtein, *V(cb) from OPE sum rules for heavy flavor transitions*, *Phys. Rev.* **D 51** (1995) 2217 [*Erratum ibid.* **D 52** (1995) 3149] [hep-ph/9405207] [INSPIRE].

[25] I.I.Y. Bigi, M.A. Shifman, N.G. Uraltsev and A.I. Vainshtein, *Sum rules for heavy flavor transitions in the SV limit*, *Phys. Rev.* **D 52** (1995) 196 [hep-ph/9405410] [INSPIRE].

[26] A. Czarnecki, K. Melnikov and N. Uraltsev, *Complete $O(\alpha_S^2)$ corrections to zero recoil sum rules for $B \to D^*$ transitions*, *Phys. Rev.* **D 57** (1998) 1769 [hep-ph/9706311] [INSPIRE].

[27] T. Mannel and D. van Dyk, *Zero-recoil sum rules for $\Lambda_b \to \Lambda_c$ form factors*, *Phys. Lett.* **B 751** (2015) 48 [arXiv:1506.08780] [INSPIRE].

[28] P. Gambino, T. Mannel and N. Uraltsev, *$B \to D^*$ Zero-Recoil Formfactor and the Heavy Quark Expansion in QCD: A Systematic Study*, *JHEP* **10** (2012) 169 [arXiv:1206.2296] [INSPIRE].

[29] Particle Data Group collaboration, C. Patrignani et al., *Review of Particle Physics*, *Chin. Phys.* **C 40** (2016) 100001 [INSPIRE].

[30] C. Bobeth, G. Hiller and G. Piranishvili, *Angular distributions of $\bar{B} \to \bar{K}\ell^+\ell^-$ decays*, *JHEP* **12** (2007) 040 [arXiv:0709.4174] [INSPIRE].

[31] LHCb collaboration, *Measurement of the b-quark production cross-section in 7 and 13 TeV pp collisions*, *Phys. Rev. Lett.* **118** (2017) 052002 [arXiv:1612.05140] [INSPIRE].

[32] LHCb collaboration, *Framework TDR for the LHCb Upgrade: Technical Design Report*, CERN-LHCC-2012-007.

[33] T. Sjöstrand, S. Mrenna and P.Z. Skands, *PYTHIA 6.4 Physics and Manual*, *JHEP* **05** (2006) 026 [hep-ph/0603175] [INSPIRE].

[34] T. Sjöstrand, S. Mrenna and P.Z. Skands, *A Brief Introduction to PYTHIA 8.1*, *Comput. Phys. Commun.* **178** (2008) 852 [arXiv:0710.3820] [INSPIRE].

[35] LHCb collaboration, *LHCb VELO (VErtex LOcator): Technical Design Report*, CERN-LHCC-2001-011.

[36] G. Ciezarek, A. Lupato, M. Rotondo and M. Vesterinen, *Reconstruction of semileptonically decaying beauty hadrons produced in high energy pp collisions*, *JHEP* **02** (2017) 021 [arXiv:1611.08522] [INSPIRE].

[37] D. Bigi, P. Gambino and S. Schacht, *$R(D^*)$, $|V_{cb}|$ and the Heavy Quark Symmetry relations between form factors*, *JHEP* **11** (2017) 061 [arXiv:1707.09509] [INSPIRE].

[38] H.E. Haber, *Spin formalism and applications to new physics searches*, hep-ph/9405376 [INSPIRE].

JHEP06(2018)155